

Report No. UT- 11.08

GFRP REINFORCED LIGHTWEIGHT PRECAST BRIDGE DECK

Prepared For:

Utah Department of Transportation
Research Division

Submitted By:

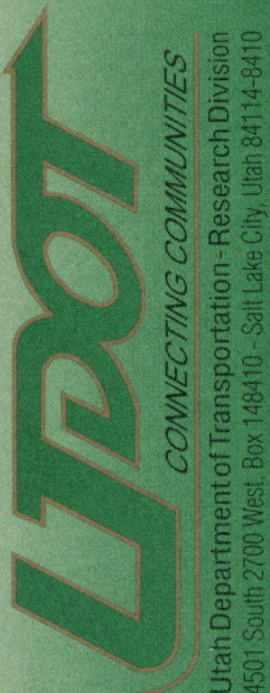
University of Utah
Department of Civil & Environmental
Engineering

Authored By:

Chris P. Pantelides, Ph.D., S.E.
Ruifen Liu, M.S.

March, 2011

RESEARCH



INSIDE COVER

Report No. UT-11.08

**GFRP REINFORCED
LIGHTWEIGHT PRECAST
BRIDGE DECK PANELS**

Prepared For:

Utah Department of Transportation
Research Division

Submitted By:

University of Utah
Department of Civil & Environmental
Engineering

Authored By:

Chris P. Pantelides, Ph.D., S.E.
Ruifen Liu, M.S.

March, 2011

THIS PAGE INTENTIONALLY LEFT BLANK

DISCLAIMER

“The authors alone are responsible for the preparation and accuracy of the information, data, analysis, discussions, recommendations, and conclusions presented herein. The contents do not necessarily reflect the views, opinions, endorsements, or policies of the Utah Department of Transportation and the US Department of Transportation. The Utah Department of Transportation makes no representation or warranty of any kind, and assumes no liability therefore.”

THIS PAGE INTENTIONALLY LEFT BLANK

Technical Report Documentation Page

1. Report No. UT-11.08		2. Government Accession No.		3. Recipient's Catalog No.	
4. Title and Subtitle GFRP REINFORCED LIGHTWEIGHT PRECAST BRIDGE DECK PANELS				5. Report Date March, 2011	
				6. Performing Organization Code	
7. Author Chris P. Pantelides, Ruifen Liu				8. Performing Organization Report No.	
9. Performing Organization Name and Address University of Utah Department of Civil and Environmental Engineering 110 S. Central Campus Dr., Room 2115 Salt Lake City, Utah 84112				10. Work Unit No. 5H06480H	
				11. Contract or Grant No. 09-9097	
12. Sponsoring Agency Name and Address Utah Department of Transportation 4501 South 2700 West Salt Lake City, Utah 84114-8410				13. Type of Report & Period Covered FINAL	
				14. Sponsoring Agency Code UT08-801	
16. Abstract <p>The present research project investigates lightweight and normal weight concrete precast panels for highway bridge decks. The deck panels are reinforced with Glass Fiber Reinforced Polymer (GFRP) bars. Due to the lack of research on lightweight concrete members reinforced with GFRP bars, the AASHTO LRFD Bridge Design Guide Specifications for GFRP Reinforced Concrete Decks do not permit the use of lightweight concrete when GFRP bars are used as flexural reinforcement. The ACI 440.1R-06 design guidelines do not provide any design information regarding the use of lightweight concrete reinforced with GFRP bars. In this research, the experimental performance of lightweight concrete versus normal weight concrete precast GFRP reinforced deck panels is investigated in terms of flexural capacity, panel deflections, and shear capacity.</p>					
17. Key Words GFRP bars; bridge deck; deck span; normal weight concrete; lightweight concrete; shear strength.			18. Distribution Statement UDOT Research Division 4501 South 2700 West Salt Lake City Utah 84114-8410		23. Registrant's Seal
19. Security Classification Unclassified	20. Security Classification Unclassified	21. No. of Pages 69	22. Price		

THIS PAGE INTENTIONALLY LEFT BLANK

ACKNOWLEDGEMENTS

The research reported in this report was supported by the Utah DOT. The authors acknowledge the contributions of the Expanded Shale Clay and Slate Institute, Hughes Bros Inc., Utelite Corporation, and Hanson Structural Precast, and the assistance of Professor Lawrence D. Reaveley, Mark Bryant, Brandon T. Besser, and Clayton A. Burningham of the University of Utah in the experimental portion of the research.

THIS PAGE INTENTIONALLY LEFT BLANK

TABLE OF CONTENTS

DISCLAIMER	i
UDOT RESEARCH & DEVELOPMENT REPORT ABSTRACT	ii
ACKNOWLEDGEMENTS	iv
EXECUTIVE SUMMARY	xii
1.0 INTRODUCTION	15
2.0 RESEARCH METHOD.....	19
2.1 Concrete Mix Design	19
2.2 Design of Experimental Specimens	19
3.0 DATA COLLECTION	27
4.0 DATA EVALUATION	31
4.1 Split Cylinder Tests.....	31
4.2 Strains in GFRP Bars and Concrete of the Panels	31
4.2 Shear Strength of Deck Panels.....	35
4.2.1 Shear Prediction from Different Codes or Research.....	35
4.2.2 Failure Mode and Experimental Shear Strength of Panels	38
4.2.3 Recommendation for Modification of the ACI 440.1R-06 Shear Equation.....	42
4.3 Deflection of Deck Panels.....	46
4.3.1 Deflection Prediction in ACI 440.1R-06	46
4.3.2 Deflection Requirements in the AASHTO LRFD Bridge Design Specifications.....	48
5.0 CONCLUSIONS.....	53
6.0 RECOMMENDATIONS AND IMPLEMENTATION.....	55
APPENDIX A. LIGHTWEIGHT CONCRETE MIX DESIGN.....	57
APPENDIX B. PROPERTIES OF SLABS USED FOR DETERMINATION OF λ	58
APPENDIX C. COMPARISON AND VERIFICATION OF DIFFERENT SHEAR PREDICTION EQUATIONS	59

APPENDIX D. DEFLECTION OF PANELS AT SERVICE AND ULTIMATE LOAD	60
REFERENCES	61
ACRONYMS.....	65

LIST OF FIGURES

Figure 1. Split-cylinder test.....	20
Figure 2. Theoretical moment-curvature relationships for reinforced concrete sections.....	21
Figure 3. Precast GFRP reinforced concrete panel with 8 ft girder spacing.....	24
Figure 4. Precast GFRP reinforced concrete panel with 9 ½ ft girder spacing.....	24
Figure 5. 6 ft wide precast GFRP reinforced concrete panel.....	25
Figure 6. Test setup.....	28
Figure 7. Loading procedure for GFRP reinforced panels.....	29
Figure 8. Strain gauges for 8 ft girder spacing GFRP reinforced panels.....	29
Figure 9. Strain gauges for 9 ½ ft girder spacing GFRP reinforced panels.....	29
Figure 10. Strain gauges for 6 ft wide GFRP reinforced panels.....	30
Figure 11. LVDTs on 2 ft wide GFRP reinforced panel.....	30
Figure 12. Split-cylinder test setup.....	32
Figure 13. GFRP bar strains in the transverse direction (perpendicular to traffic direction) for panel 5-NW-B2.....	33
Figure 14. GFRP bar strains in the longitudinal direction (parallel to traffic direction) for panel 5-NW-B2.....	33
Figure 15. Concrete strains on the top face of panel 5-NW-B2.....	34
Figure 16. Diagonal tension failure of 6 ft wide specimen.....	35
Figure 17. Load deflection diagram for 2 ft x 12 ft specimens.....	39
Figure 18. Load deflection diagram for 2 ft x 13 ½ ft specimens.....	40
Figure 19. Load deflection diagram for 6 ft x 12 ft specimens.....	41
Figure 20. Failure of 2 ft wide panels: (a) NW GFRP panel, (b) LW GFRP panel.....	41
Figure 21. Failure of 6 ft wide panels: (a) NW GFRP panel, (b) LW GFRP panel.....	42
Figure 22. Experimental shear strength normalized by ACI 440 equation.....	45
Figure 23. Experimental shear strength normalized by modified equation Eq. (12).....	45
Figure 24. Deflection prediction.....	48
Figure 25. Deflection requirement under service moment for 2 ft x 12 ft panels.....	49
Figure 26. Deflection requirement under service moment for 2 ft x 13 ½ ft panels.....	50
Figure 27. Deflection requirement under service moment for 6 ft x 12 ft panels.....	50
Figure 28. Deflection requirement under service moment: comparison of 2 ft x 12 ft panels with 2 ft x 13 ½ ft panels.....	51

THIS PAGE INTENTIONALLY LEFT BLANK

LIST OF TABLES

Table 1. Matrix of Test Specimens	23
Table 2. Tensile Splitting Strength	32
Table 3. Summary of Test Results	39
Table 4. Deflection of Panels at Service and Ultimate Load	48
Table 5. Deflection under Service Load Moment Compared to the AASHTO LRFD Bridge Design Specifications.....	52

THIS PAGE INTENTIONALLY LEFT BLANK

EXECUTIVE SUMMARY

The present research project investigates lightweight and normal weight concrete precast panels for highway bridge decks. The deck panels are reinforced with GFRP bars. Due to the lack of research on lightweight concrete members reinforced with GFRP bars, the AASHTO LRFD Bridge Design Guide Specifications for GFRP Reinforced Concrete Decks (AASHTO 2009) do not permit the use of lightweight concrete when GFRP bars are used as flexural reinforcement. The ACI 440.1R (ACI 2006) guidelines do not provide any design information regarding the use of lightweight concrete reinforced with GFRP bars. In this research, the experimental performance of lightweight concrete precast GFRP reinforced deck panels versus normal weight concrete precast GFRP reinforced deck panels is investigated in terms of flexural capacity, panel deflections, and shear capacity. Shorter girder spacing has been used for bridge deck construction to limit deflections because of the lower modulus of elasticity of GFRP bars compared to steel bars. A typical girder spacing of 9 ½ ft for steel reinforced deck panels, as well as a narrower girder spacing of 8 ft have been used in the design of the specimens tested in this research; the performance of the GFRP panels for both girder spacings is compared. The applicability of existing equations in the ACI 440.1R (2006) design guidelines when members are reinforced with GFRP bars and constructed using lightweight concrete is evaluated, and some modifications are suggested for design, based on the test results. Using GFRP bars properties provided by the manufacturer, normal weight concrete deck panels reinforced with GFRP bars achieved 1.90 to 2.10 times the shear capacity predicted by the ACI 440.1R-06 one-way shear equation. Using a reduction factor λ of 0.80, the average of the ratio of experimental shear strength to that predicted using the modified equation is 1.88 for lightweight concrete panels, which is in line with the capacity achieved by the normal weight panels. The 9½ ft deck span panels with a 10 ¾ in. thickness worked equally well compared to the 8 ft deck span panels with a 9 ¼ in. thickness. Under service load, both 9½ ft span panels with a 10 ¾ in. thickness and 8 ft span panels with a 9 ¼ in. thickness satisfied the AASHTO LRFD Bridge Design Specifications (2007) deflection requirements.

THIS PAGE INTENTIONALLY LEFT BLANK

1.0 INTRODUCTION

Corrosion of steel is a major cause of deterioration of reinforced concrete structures. Concrete bridge decks are subjected to severe environmental conditions such as use of deicing salts, significant variations in temperature, and multiple freeze-thaw cycles. As an example, from 1948 until 2000, Salt Lake City had an average of 103 freeze-thaw cycle days per year. Concrete bridge decks have an average life of 35 to 40 years mainly because of deterioration due to corrosion of steel reinforcement. The expansion of steel reinforcement due to corrosion causes the concrete bridge deck to experience cracking and spalling; this results in major rehabilitation costs and traffic disruption (Yunovich and Thompson 2003). Fiber Reinforced Polymer (FRP) bars are immune to chloride-induced corrosion, and have higher tensile strength compared to steel bars. The noncorrosive FRP bar provides a viable alternative to steel as reinforcement for concrete bridge decks under severe corrosion conditions. Glass Fiber Reinforced Polymer (GFRP) is more economical compared to Carbon Fiber Reinforced Polymer (CFRP) or Aramid Fiber Reinforced Polymer (AFRP), and is generally used in bridge decks as an alternative to steel reinforcement.

Lightweight concrete has approximately 75%-85% the weight of normal weight concrete. Examination of a number of projects constructed with steel reinforced lightweight concrete bridge decks has demonstrated that they can perform well in service for a range of different environments (Castrodale and Robinson, 2008); this includes sites that vary from coastal with salt breezes, to mountainous where salt is applied to deice the deck in winter; in addition, traffic counts ranged from very heavy urban interstate travel with a high percentage of trucks to light rural traffic.

The use of lightweight concrete precast bridge decks reinforced with GFRP bars is cost-competitive in environments where chloride-induced deterioration is an issue and will extend the life of the deck. Several benefits could be gained from lightweight concrete precast GFRP reinforced deck panels, especially when they are used in Accelerated Bridge Construction (ABC); in this method of construction, the whole bridge or parts of the bridge are constructed

elsewhere and brought to the bridge site using mobile transportation. The reduced weight of decks constructed with lightweight concrete implies that they could be lifted with smaller cranes; in addition, the reduction in weight is beneficial for the design of the substructure and foundations since the weight of the deck is the main dead load resisted by the substructure and foundations. Use of GFRP bars is cost-competitive when life-cycle costs are considered in environments where chloride induced deterioration is an issue; this is the case in Utah where deicing salts are used in the winter. Moreover, the reduced weight of GFRP bars compared to steel bars makes them easier to handle during construction. Reduction of weight is also beneficial when seismic forces are considered.

Many design provisions and guidelines are available for the design of concrete beams or slabs reinforced with GFRP bars: these include the Japan Society of Civil Engineers Design Provisions (JSCE 1997), the Canadian Design Provisions (CAN/CSA-S806-02 2002), the American Concrete Institute Guidelines (ACI 440.1R-06 2006), and the American Association of State Highway and Transportation Officials Load Resistance Factor Design (LRFD) Bridge Design Guide Specifications for GFRP Reinforced Concrete Decks (AASHTO 2009).

Extensive research has been carried out to determine the shear capacity of GFRP reinforced beams or slabs without transverse shear reinforcement. Swamy and Aburawi (1997) evaluated the performance of concrete beams reinforced with GFRP bars and suggested that an integrated approach to design based on material and structural interaction may give engineers the breakthrough to optimum designs with GFRP bars. Deitz et al. (1999) tested several GFRP reinforced deck panels, and proposed two equations for computing the capacity of concrete panels reinforced in tension with GFRP bars failing in shear. Alkhrdaji et al. (2001) found that the contribution of concrete to internal shear resistance was influenced by the amount of longitudinal reinforcement. Yost et al. (2001) evaluated the shear strength of intermediate length simply supported concrete beams and found that shear strength was independent of the amount of longitudinal GFRP reinforcement; a simplified empirical equation for predicting the ultimate shear strength of concrete beams reinforced with GFRP bars was endorsed. Tureyen and Frosch (2002) investigated different types of FRP reinforcement and found that the ACI 440 (2001) method was very conservative, whereas the ACI 318 (1999) method resulted in unconservative

computations of shear strength. Gross et al. (2003) evaluated the shear strength for normal and high strength concrete beams and found that the longitudinal reinforcement ratio had a small influence on the concrete shear strength; in addition, high strength concrete beams exhibited a slightly lower relative shear strength than normal strength concrete beams. Ashour (2005) tested concrete beams reinforced with GFRP bars and determined that the theoretical prediction of shear capacity obtained from modifying the ACI 318-99 recommendations was inconsistent and that further research was necessary to establish a rational method for shear capacity. El-Sayed et al. (2005) investigated several full-size slabs and found that the ACI 440.1R-03 (2003) design method for predicting the shear strength of FRP slabs was very conservative; better predictions were obtained by both the Canadian CAN/CSA-S806-02 Code and the Japan Society of Civil Engineers design recommendations (JSCE 1997). El-Sayed et al. (2006a) investigated the behavior and shear strength of concrete slender beams reinforced with FRP bars and found that ACI 440.1R-03 was very conservative and proposed a modification to the ACI shear prediction. El-Sayed, et al. (2006b) reported experimental data on the shear strength of high-strength concrete slender beams and found that high-strength concrete beams exhibited slightly lower relative shear strength compared to normal-strength concrete beams. Alam and Hussein (2009) found that the shear strength of GFRP reinforced concrete beams was a function of the shear span to depth ratio, the effective depth of the beam and the longitudinal reinforcement ratio. Jang et al. (2009) proposed a shear strength correction factor to evaluate the shear strength of FRP reinforced concrete beams considering the elastic modulus of FRP reinforcement, shear span to depth ratio, and flexural reinforcement ratio. Bentz et al. (2010) summarized the results of tests for reinforced concrete beams with GFRP reinforcement and found that members with multiple layers of longitudinal bars appeared to perform better in shear capacity than those with a single layer of longitudinal reinforcing bars; in addition, they found that the fundamental shear behavior of FRP reinforced beams was similar to that of steel-reinforced beams despite the brittle nature of the reinforcement.

The present project investigates lightweight and normal weight concrete precast deck panels for highway bridges. The deck panels are reinforced with GFRP bars. Due to the lack of research on lightweight concrete members reinforced with GFRP bars, the AASHTO LRFD Bridge Design Guide Specifications for GFRP Reinforced Concrete Decks (AASHTO 2009) do

not permit the use of lightweight concrete when GFRP bars are used as flexural reinforcement. The ACI 440.1R (ACI 2006) guidelines do not provide any design information regarding the use of lightweight concrete reinforced with GFRP bars. In this research, the experimental performance of lightweight concrete precast GFRP reinforced deck panels versus normal weight concrete precast GFRP reinforced deck panels is investigated in terms of flexural capacity, panel deflections, shear capacity, and crack widths. Narrow girder spacing has been used in bridge deck construction to limit deflections because of the lower modulus of elasticity of GFRP bars compared to steel bars. Both typical girder spacing, and narrow girder spacing with different panel thickness have been used in the design of the specimens tested in this research; the performance of the GFRP panels for both girder spacings and different thickness is compared. The applicability of existing equations in the ACI 440.1R (2006) design guidelines when members are reinforced with GFRP bars and constructed using lightweight concrete is evaluated, and some modifications are suggested for design based on the test results from this research and the available literature.

2.0 RESEARCH METHOD

2.1 Concrete Mix Design

Sand lightweight concrete was used in this research. Lightweight aggregate from local producers was used to perform various mix designs for the lightweight concrete. The lightweight concrete mix design selected and used in this research is given in Appendix A. The lightweight concrete obtained from this mix design was evaluated for compressive and tensile strength. The concrete compressive strength was obtained from compression tests of 4 in. diameter by 8 in. height cylinders according to ASTM Standard C39 (ASTM 2009). The tensile strength was obtained from split-cylinder tests of 4 in. diameter by 8 in. long cylinders as shown in Figure 1; the test was performed according to ASTM Standard C496 (ASTM 2004). Figure 1 shows the split-cylinder test setup and a typical split concrete cylinder specimen.

2.2 Design of Experimental Specimens

According to ACI 440.1R-06 (ACI 2006), an FRP-reinforced concrete member is designed based on its required flexural strength and checked for shear, fatigue endurance, creep rupture endurance, and serviceability criteria. FRP reinforcement behaves in a linear elastic manner until failure. Both failure modes (FRP rupture and concrete crushing) are acceptable in governing the design of flexural members reinforced with FRP bars, provided that strength and serviceability criteria are satisfied. FRP reinforcement cannot yield, and to compensate for the lack of ductility, the member should possess a higher reserve of strength. The margin of safety suggested in the ACI 440.1R-06 guidelines against failure is higher than that used in traditional steel-reinforced concrete design. The concrete crushing failure is more desirable for flexural members reinforced with FRP bars. By experiencing concrete crushing, a flexural member exhibits some plastic behavior before failure. As shown in Figure 2, when concrete flexural members are reinforced with GFRP bars, under the same bending moment, a given



(a) test setup

(b) split concrete cylinder

Figure 1. Split-cylinder test

flexural member would experience more deformation if it fails in concrete crushing rather than GFRP bar rupture.

The flexural capacity of an FRP reinforced flexural member depends on whether failure is governed by concrete crushing or FRP rupture, which can be determined by comparing the FRP reinforcement ratio ρ_f to the balanced reinforcement ratio ρ_{fb} given as:

$$\rho_f = \frac{A_f}{bd} \quad (1a)$$

$$\rho_{fb} = 0.85\beta_1 \frac{f'_c}{f_{fu}} \frac{E_f \varepsilon_{cu}}{E_f \varepsilon_{cu} + f_{fu}} \quad (1b)$$

where ρ_f = FRP reinforcement ratio; ρ_{fb} = FRP reinforcement ratio producing balanced strain conditions; A_f = area of FRP reinforcement; b = width of rectangular cross section; d = distance from extreme compression fiber to the centroid of tension reinforcement; β_1 = factor taken as 0.85 for concrete compressive strengths up to and including 4,000 psi; for concrete compressive strengths above 4,000 psi, this factor is reduced continuously at a rate of 0.05 per each 1,000 psi

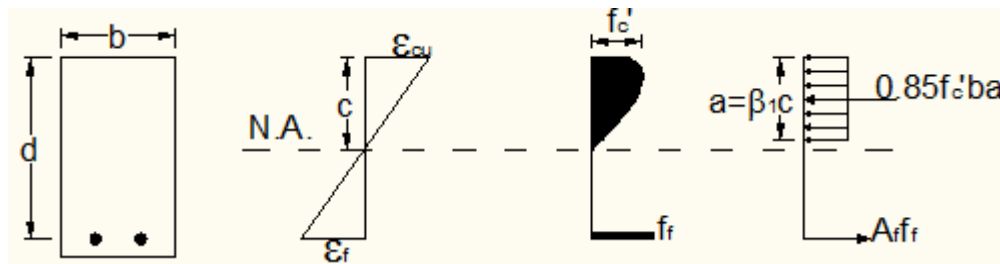
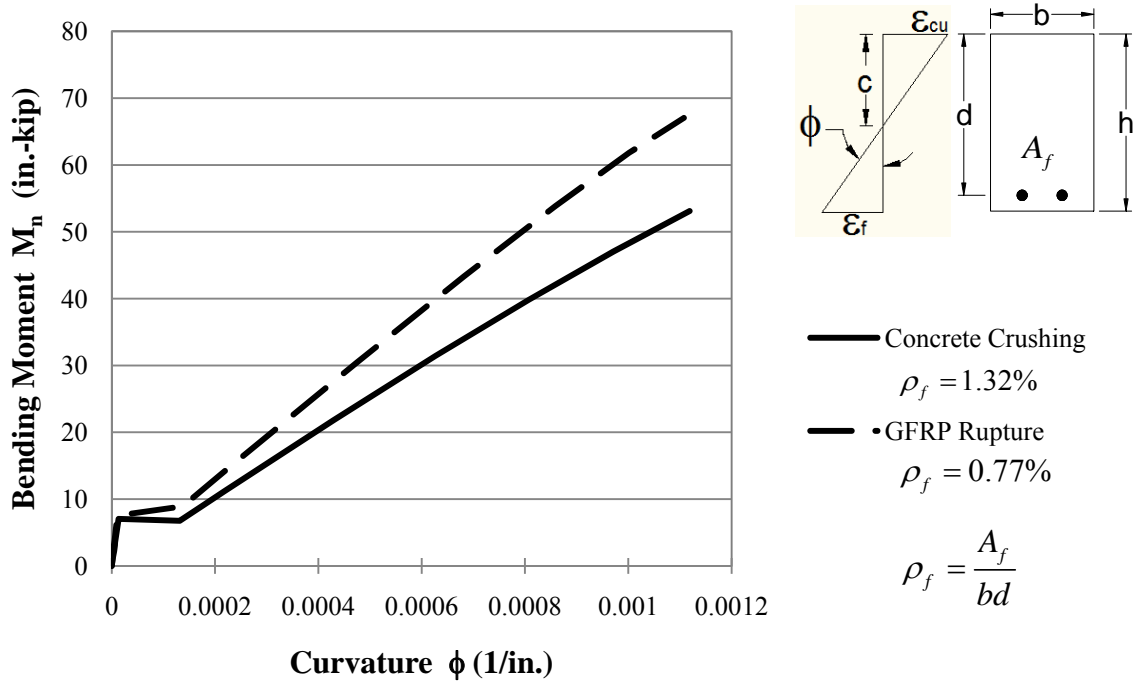


Figure 2. Theoretical moment-curvature relationships for reinforced concrete sections

of strength in excess of 4,000 psi, but is not to be taken less than 0.65; f'_c = compressive strength of concrete; ϵ_{cu} = ultimate strain in concrete; f_{fu} = design tensile strength of FRP bars considering reduction for service environment; E_f = design or guaranteed modulus of elasticity of FRP bars.

If the reinforcement ratio provided is greater than the balanced FRP reinforcement ratio, concrete crushing governs. Concrete crushing is more desirable than FRP bar rupture. The design in this research is intended to have concrete experience a crushing failure mode before FRP bar rupture. The ultimate moment capacity of flexural members is obtained as:

$$M_n = A_f f_f \left(d - \frac{a}{2} \right) \quad (2a)$$

$$a = \frac{A_f f_f}{0.85 f_c' b} \quad (2b)$$

$$f_f = E_f \varepsilon_{cu} \left(\frac{\beta_1 d - a}{a} \right) \quad (3)$$

where M_n = nominal moment capacity; A_f = area of FRP reinforcement; f_f = stress in FRP reinforcement in tension.

The specimens tested in this research were designed according to the flexural design method and then checked for shear strength according to ACI 440.1R-06. The shear capacity according to ACI 440.1R-06 is given as:

$$V_c = 5\sqrt{f_c'} b_w c \quad (4a)$$

$$c = kd \quad (4b)$$

$$k = \sqrt{2\rho_f n_f + (\rho_f n_f)^2} - \rho_f n_f \quad (4c)$$

where c = cracked transformed section neutral axis depth; d = distance from extreme compression fiber to neutral axis; n_f = ratio of modulus of elasticity of FRP bars to modulus of elasticity of concrete; k = ratio of depth of neutral axis to reinforcement depth. Six specimens were designed according to the flexural design method. The experiments are described in Table 1. Three lightweight concrete panels and three normal weight concrete panels were constructed.

For the specimen description in Table 1, the first number is the specimen number; NW means normal weight concrete; LW means lightweight concrete; B1 means the specimen was cast using the first batch of concrete, B2 means the specimen was cast using the second batch of concrete.

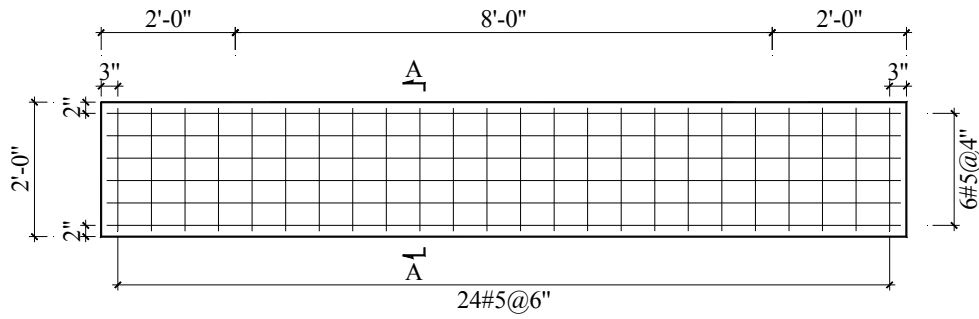
All specimens were reinforced with GFRP bars in an identical manner. The reinforcement provided is as follows: The top and bottom transverse bars (which make up the main

reinforcement transverse to the traffic direction) are #5@4 in. The bottom distribution bars are #5@6 in., and the top temperature and shrinkage reinforcement bars are also #5@6 in. The reinforcement diagram for the 8 ft girder spacing precast concrete GFRP reinforced panels with the 9 ¼ in. thickness is shown in Figure 3. The GFRP reinforcement diagram for the 9 ½ ft girder spacing precast concrete panels with 10 ¾ in. thickness is shown in Figure 4. The reinforcement diagram for the 6 ft wide precast concrete panels with 8 ft girder spacing and 9 ¼ in. thickness is shown in Figure 5. The properties of the GFRP bars were obtained online from the manufacturer’s website as follows: E_f = modulus of elasticity (5,920,000 psi); f_{fu} = design tensile strength of GFRP bars (95,000 psi); ϵ_{fu} = design rupture strain of GFRP bars (1.6%). The actual properties of the GFRP bars were also provided by the manufacturer for the specific batch used in this research, as follows: E_f = modulus of elasticity (6,279,618 psi); f_{fu} = design tensile strength of GFRP bars (103,674 psi); ϵ_{fu} = design rupture strain of GFRP bars (1.45%).

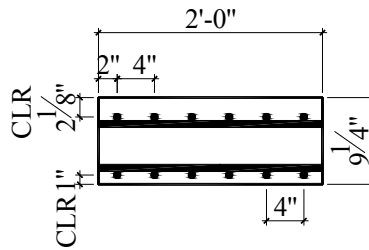
Table 1. Matrix of Test Specimens

Specimen	*Concrete Strength (psi)	Slab Thickness (in.)	Girder Spacing (ft)	Specimen Dimension (ft X ft)
1-NW-B2	8,760	9 ¼	8	2’X12’
2-LW-B1	10,930	9 ¼	8	2’X12’
3-NW-B2	8,840	10 ¾	9 ½	2’X13.5’
4-LW-B2	8,460	10 ¾	9 ½	2’X13.5’
5-NW-B2	8,510	9 ¼	8	6’X12’
6-LW-B1	9,080	9 ¼	8	6’X12’

*Concrete compressive strength at the time of testing.

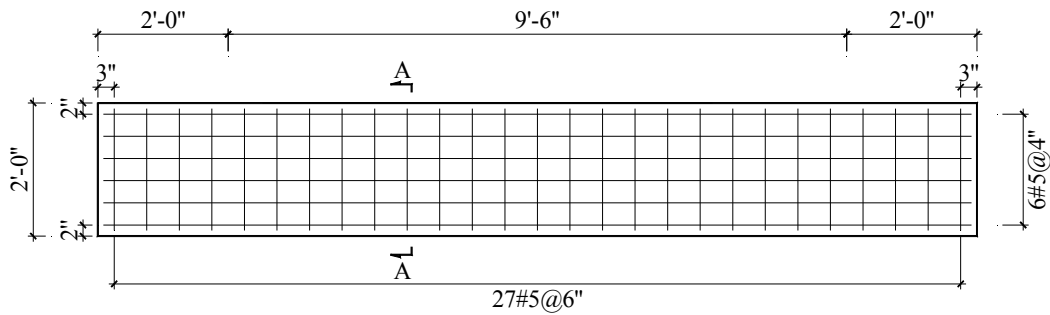


Top and Bottom Reinforcement

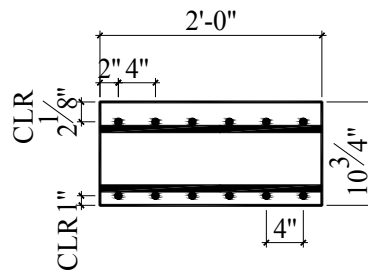


Section A-A

Figure 3. Precast GFRP reinforced concrete panel with 8 ft girder spacing

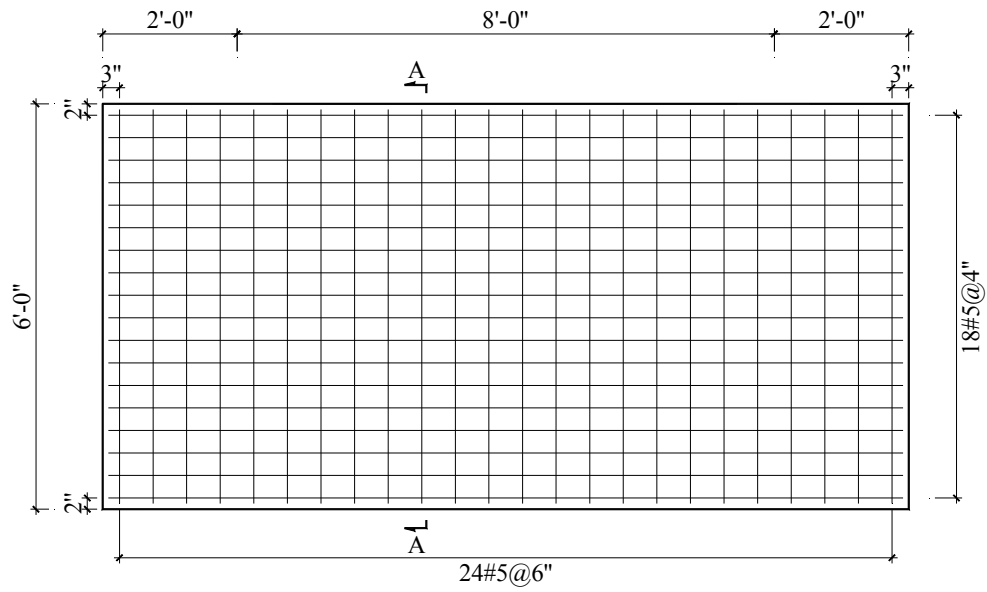


Top and Bottom Reinforcement

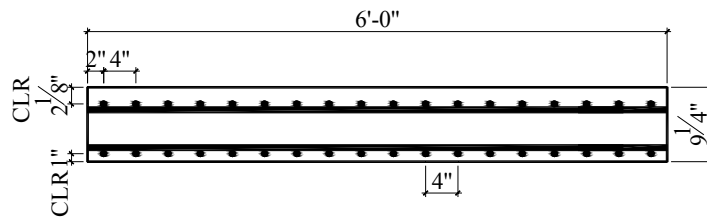


Section A-A

Figure 4. Precast GFRP reinforced concrete panel with 9 1/2 ft girder spacing



Top and Bottom Reinforcement



Section A-A

Figure 5. 6 ft wide precast GFRP reinforced concrete panel

THIS PAGE INTENTIONALLY LEFT BLANK

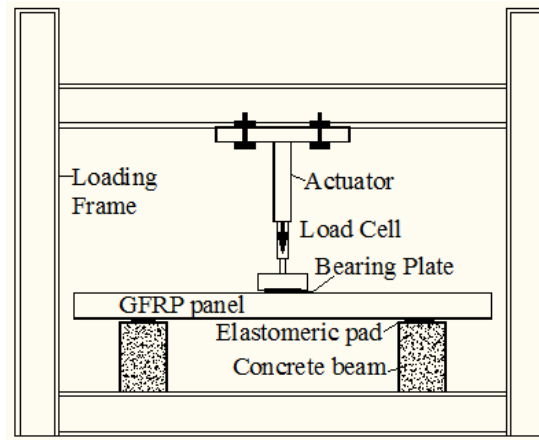
3.0 DATA COLLECTION

The existing load frame at the University of Utah Structures Laboratory was used to perform the experiments. The test setup is shown in Figure 6. The precast deck panels were simply supported on two reinforced concrete beams. The reinforced concrete beams were 20 in. high, 2 ft wide and 6 ft long. Two elastomeric pads were placed between the concrete beams and the panels, to allow the panels to rotate freely. Each panel was loaded using a steel bearing plate with a contact area equal to 10 in. x 20 in., which is equivalent to the contact area of a double tire wheel load, as specified in the AASHTO LRFD Bridge Design Specifications (2007). The experiments were carried out using displacement controlled loading; the load was applied using a hydraulic actuator. Each deck panel was subjected to compression only cycles without stress reversals with the displacement increasing during each cycle; the rate of loading was 0.2 in./min and the loading procedure is shown in Figure 7.

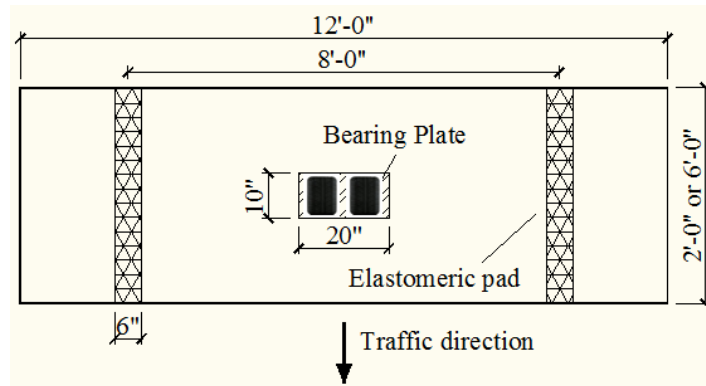
Quantities to be measured included strains in the GFRP bars located on the top and bottom GFRP mat; strains at the top face of the concrete section; deflections of the panel at midspan and quarter span points; applied load. Electrical strain gauges on the bottom GFRP mat for the 8 ft wide girder spacing precast GFRP reinforced concrete panels are shown in Figure 8; strain gauges on the bottom GFRP mat for the 9 ½ ft wide girder spacing precast GFRP reinforced concrete panels are shown in Figure 9; strain gages on the bottom GFRP mat for the 6 ft wide precast GFRP reinforced concrete panels are shown in Figure 10. In Figures 8-10, the dashed rectangular boxes represent the strain gauges applied on the top face of the concrete panels.

Linear Variable Displacement Transducers (LVDT) were used at mid-span and at the two quarter points to measure vertical displacements during testing of the 2 ft wide specimens, as shown in Figure 11; for the 6 ft wide specimens, two more LVDTs were added in the mid-span on each side of the specimen.

All data was collected using a 16 bit data acquisition system, including strains from strain gauges and deflections from LVDTs. The actuator load was measured using a load cell and the actuator displacement was collected using a dedicated external LVDT.



ELEVATION



PLAN

Figure 6. Test setup

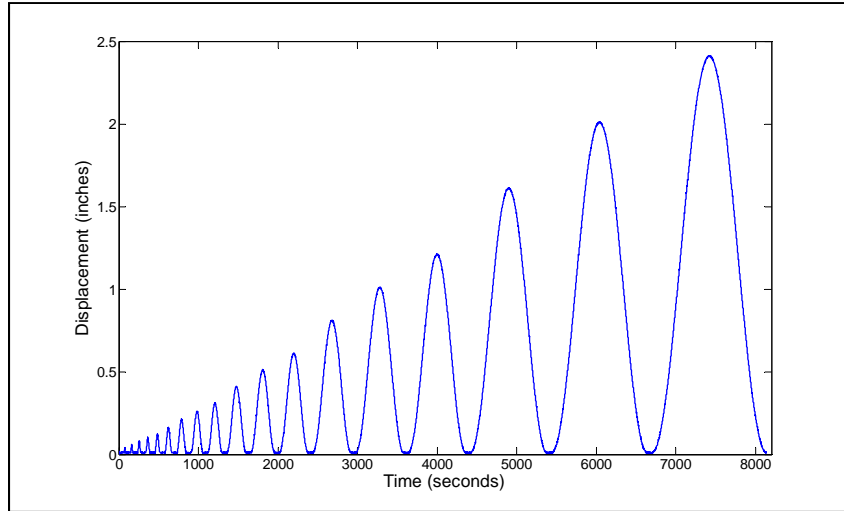


Figure 7. Loading procedure for GFRP reinforced panels

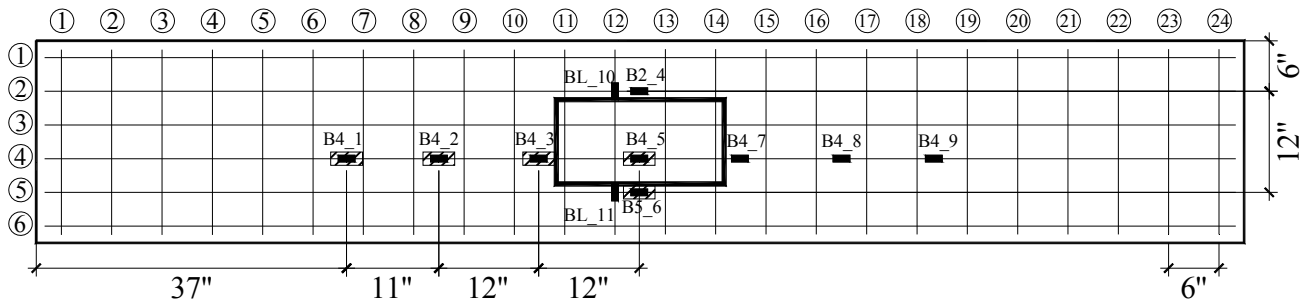


Figure 8. Strain gauges for 8 ft girder spacing GFRP reinforced panels

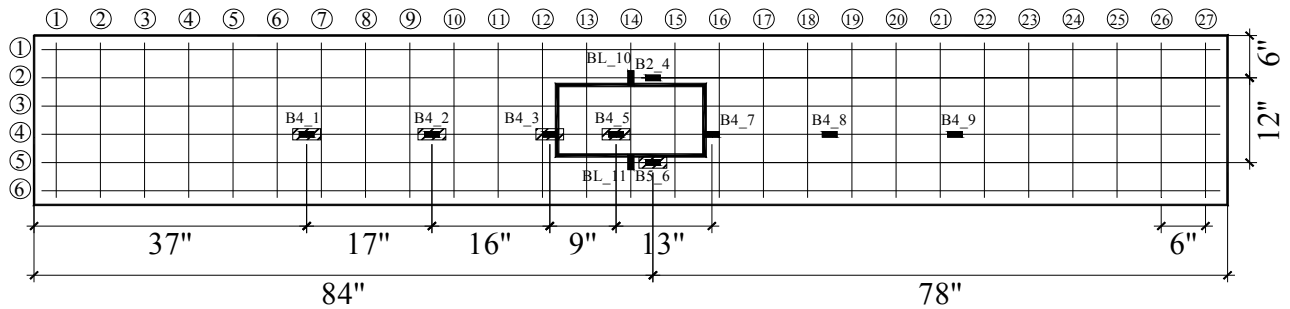


Figure 9. Strain gauges for 9 1/2 ft girder spacing GFRP reinforced panels

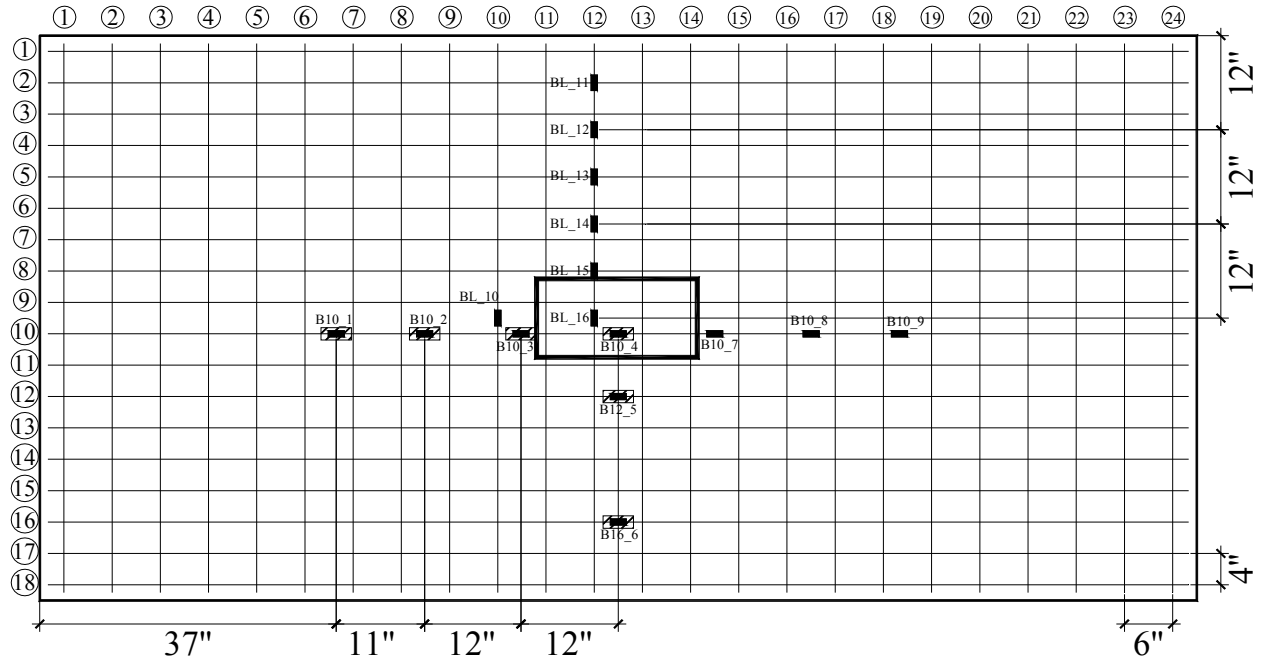


Figure 10. Strain gauges for 6 ft wide GFRP reinforced panels

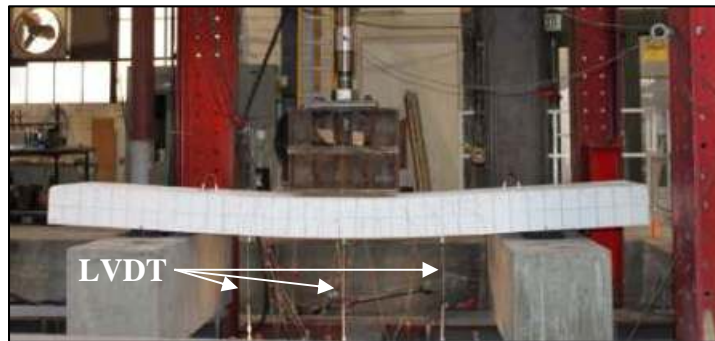


Figure 11. LVDTs on 2 ft wide GFRP reinforced panel

4.0 DATA EVALUATION

4.1 Split Cylinder Tests

Split cylinder tests were carried out to obtain the tensile splitting strength of concrete f_t according to ASTM C496/C 496M-04 (ASTM 2004). The test consists of applying a diametral compressive force along the length of a cylindrical concrete specimen, as described in Section 3.0. Thin plywood bearing strips are used to distribute the applied load evenly along the length of the cylinder, as shown in Figure 12. The maximum load sustained by the cylindrical concrete specimen is divided by appropriate geometrical factors to obtain the tensile splitting strength. The results of the tests are shown in Table 2. The tensile splitting strength of the cylindrical concrete specimen is given as:

$$f_t = \frac{2P}{\pi Ld} \quad (5)$$

where f_t = tensile splitting strength, (psi); P = maximum applied load indicated by the testing machine, (lbs); L = length, (in.); d = diameter, (in.).

The average tensile splitting strength of lightweight concrete was measured as $5.00\sqrt{f'_c}$ and that of normal weight concrete as $5.52\sqrt{f'_c}$; thus, the lightweight concrete used has a tensile splitting strength equal to 90% of the normal weight concrete tensile splitting strength.

4.2 Strains in GFRP Bars and Concrete of the Panels

Strains in the bars on the bottom GFRP mat of the deck panels and strains in the concrete at the top face of the panels were collected using the data acquisition system; the location of the strain gauges for the 6 ft wide panels is shown in Figure 10. Figure 13 shows the strains collected from strain gauges in the transverse direction (perpendicular to the direction of traffic) for the 6 ft x 12 ft specimen 5-NW-B2; Figure 14 shows the strains collected in the longitudinal

direction (along the direction of traffic). Figure 15 shows the strains collected on the top face of the concrete panel (the strain gauge locations correspond to Figure 10; concrete strain gauges #1-#5 are numbered from left to right).

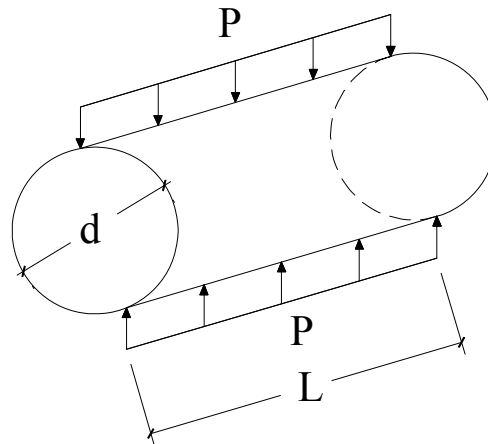


Figure 12. Split-cylinder test setup

Table 2. Tensile Splitting Strength

Date	Cylindrical Specimen	f'_c (psi)	Load (lbs)	Tensile Stress (psi)	Normalized Tensile Strength $f_t/\sqrt{f'_c}$	Average
8-Jun-09	LW #1	8,600	32,406	644.70	6.95	5.13
	LW #2	8,600	23,409	465.70	5.02	
	LW #3	8,600	16,193	322.15	3.47	
13-Mar-09	NW #1	11,700	28,899	574.93	5.32	5.52
	NW #2	11,700	31,112	618.95	5.72	
13-Mar-09	LW #1	10,900	26,628	529.75	5.07	4.66
	LW #2	10,900	26,820	533.57	5.11	
	LW #3	10,900	19,893	395.76	3.79	
11-Mar-09	LW #1	9,100	21,228	422.32	4.43	4.28
	LW #2	9,100	16,954	337.29	3.54	
	LW #3	9,100	23,333	464.20	4.87	
10-Mar-09	LW #1	12,100	32,276	642.11	5.84	5.91
	LW #2	12,100	35,069	697.68	6.34	
	LW #3	12,100	30,620	609.17	5.54	

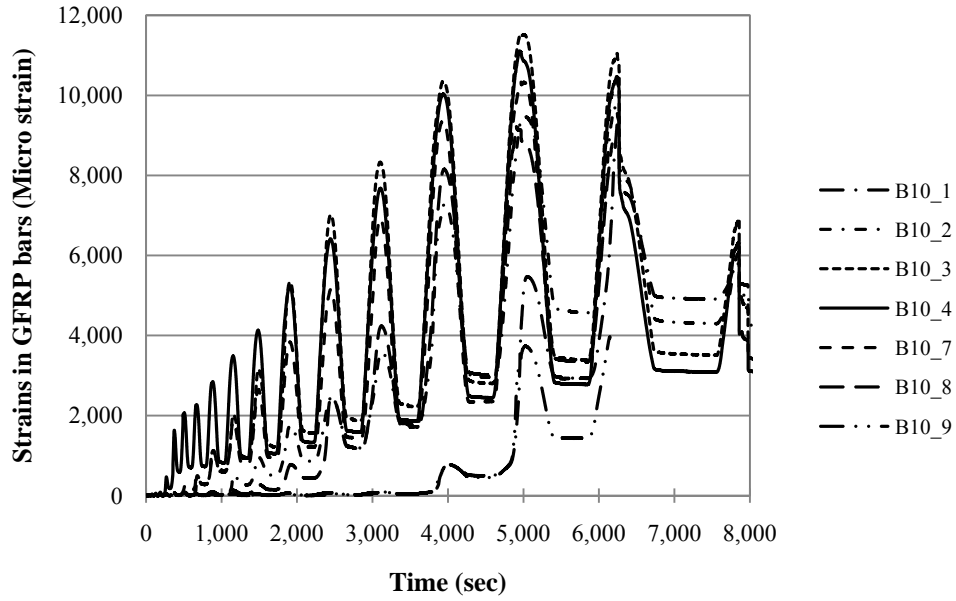


Figure 13. GFRP bar strains in the transverse direction (perpendicular to traffic direction) for panel 5-NW-B2

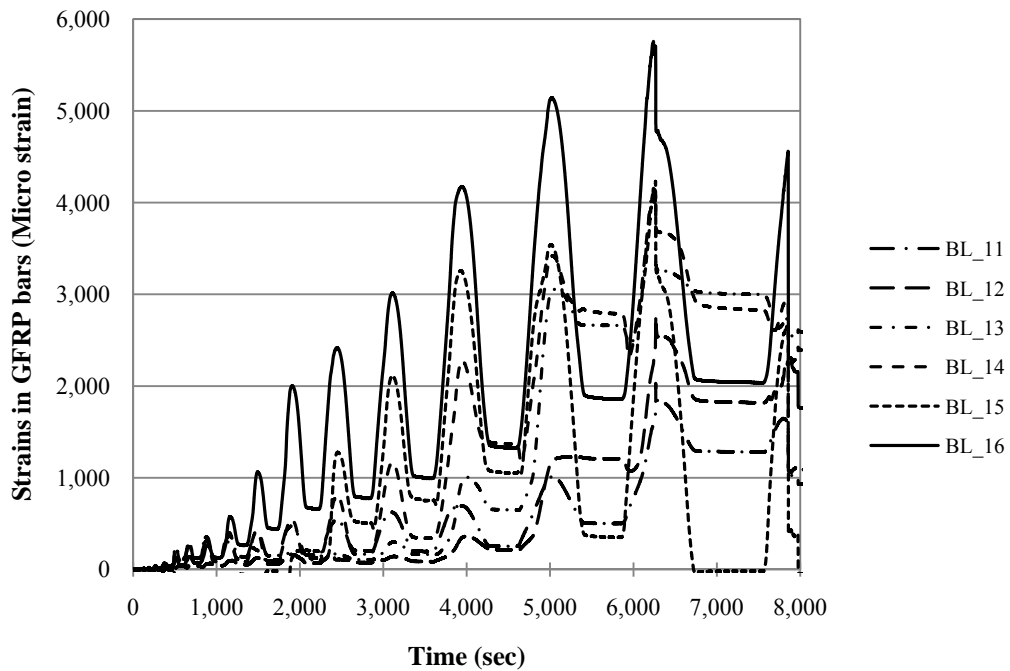


Figure 14. GFRP bar strains in the longitudinal direction (parallel to traffic direction) for panel 5-NW-B2

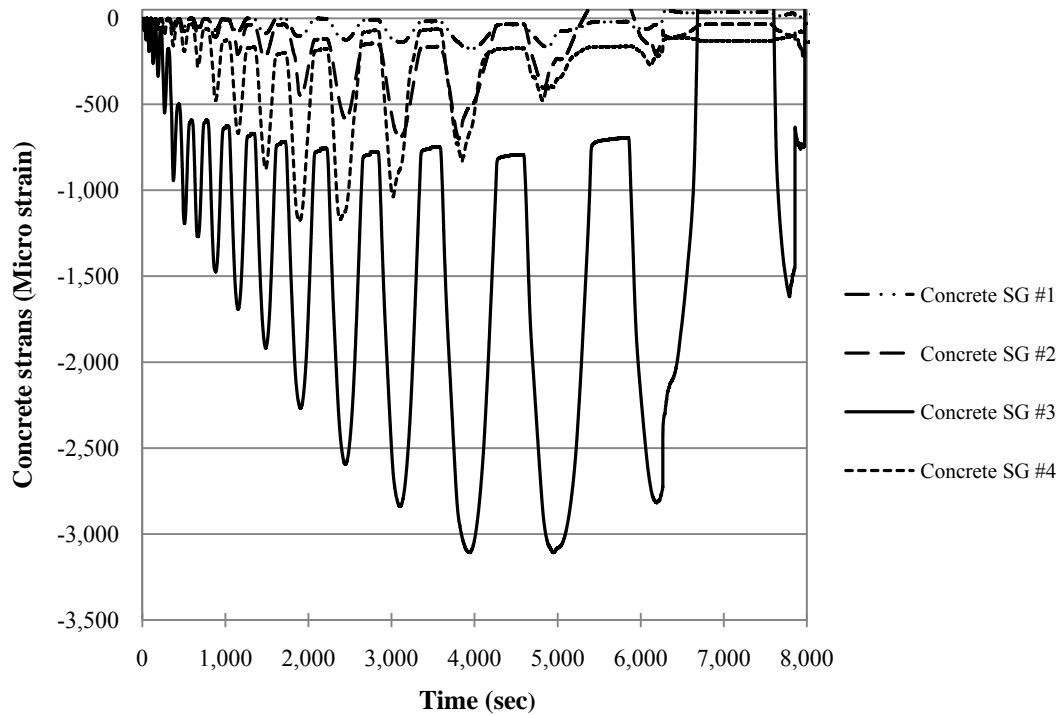


Figure 15. Concrete strains on the top face of panel 5-NW-B2

Figure 13 shows that the highest strain in the GFRP bars occurred in strain gauge B10_3, which is near the edge of the load bearing steel plate. Strains were higher on the perimeter of the bearing plate than the strain at the center of the steel plate. Strain gauges which had symmetric positions recorded similar measured strains. GFRP bar strains were smaller near the panel support. The maximum tensile strain measured was 11,450 microstrains which is approximately 70% of the ultimate tensile strain of the GFRP bar. This agrees with visual evidence that none of the GFRP bars failed in tension. Figure 14 shows strains along the longitudinal direction of the panels. The strains are approximately one half those measured in the GFRP bars along the transverse direction shown in Figure 13. Strains in both figures become higher as the strain gauge position approaches the midspan of the panels. Figure 15 shows strains in the concrete at the top face of the panel. The figure shows that the highest strain in the concrete occurs near the perimeter of the load bearing plate. The maximum compressive strain measured was 3,100 microstrains. This agrees with visual evidence that at failure concrete reached its compressive strain capacity and crushed. However, the measured strains in concrete and GFRP bars vary according to the specimen; some specimens had higher strains in the GFRP bar than measured in the 5-NW-B2 specimen.

4.2 Shear Strength of Deck Panels

All specimens tested failed in a diagonal tension failure mode. The concrete was horizontally split along the longitudinal reinforcement shortly after the formation of the critical diagonal crack. Figure 16 shows this failure mode which occurred suddenly but not catastrophically. None of the GFRP bars on the bottom mat ruptured in tension in any of the tests. However, a small number of top mat GFRP bars near the edge of a few specimens snapped and sheared off after the ultimate load was reached, shortly before the ultimate deflection. All specimens tested (normal weight and lightweight concrete) had a compressive strength higher than 6,000 psi, as shown in Table 1, and are considered to be high strength concrete. To check the validity of the diagonal tension failure mode leading to the ultimate shear capacity, several different codes and proposed equations from other research are described.

4.2.1 Shear Prediction from Different Codes or Research

a) American Concrete Institute Guidelines (ACI 440.1R-06 2006)

The one-way shear capacity V_c for GFRP reinforced concrete members is given as:

$$V_c = 5\sqrt{f'_c}b_w c \quad (\text{lbs})$$

$$V_c = \frac{2}{5}\sqrt{f'_c}b_w c \quad (\text{kN}) \quad (6a)$$

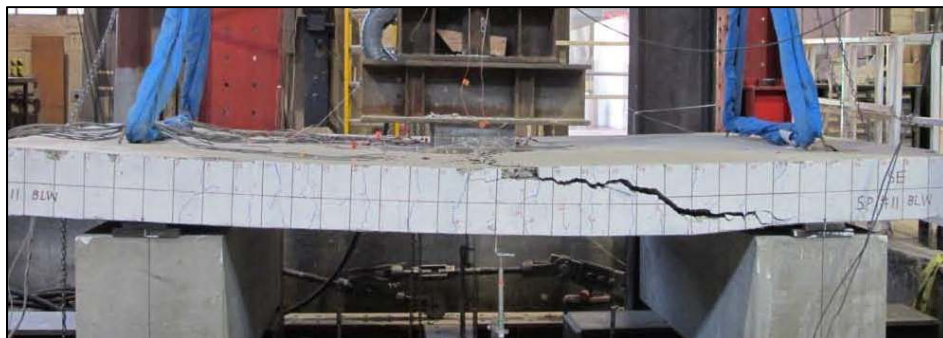


Figure 16. Diagonal tension failure of 6 ft wide specimen

$$c = kd \quad (6b)$$

$$k = \sqrt{2\rho_f n_f + (\rho_f n_f)^2} - \rho_f n_f \quad (6c)$$

where f'_c = specified compressive strength of concrete; c = cracked transformed section neutral axis depth; d = distance from extreme compression fiber to centroid of tension reinforcement; n_f = ratio of modulus of elasticity of FRP bars to modulus of elasticity of concrete; k = ratio of depth of neutral axis to reinforcement depth.

b) Japan Society of Civil Engineer Design Provisions (JSCE 1997):

The Japan Society of Civil Engineers has published design provisions for shear design; the shear capacity (for one-way shear) is given in SI units as:

$$V_c = \beta_d \beta_p \beta_n f_{vcd} b_w d / \gamma_b \quad (7a)$$

$$f_{vcd} = 0.2 (f'_{cd})^{1/3} \leq 0.72 \text{ N/mm}^2 \quad (7b)$$

$$\beta_d = (1000/d)^{1/4} \leq 1.5 \quad (7c)$$

$$\beta_p = (100\rho_f E_f / E_s)^{1/3} \leq 1.5 \quad (7d)$$

$$\beta_n = 1 + M_o / M_d \leq 2 \quad \text{for } N'_d \geq 0 \quad (7e)$$

$$\beta_n = 1 + 2M_o / M_d \geq 0 \quad \text{for } N'_d < 0 \quad (7f)$$

where γ_b = member safety factor ($\gamma_b=1.3$); f'_{cd} = concrete design compressive strength;

E_s = modulus of elasticity of steel; M_o = decompression moment; M_d = design bending moment;

N'_d = design axial compressive force.

c) Canadian Design Provisions (CAN/CSA-S806-02 2002)

The concrete contribution to shear strength is calculated using the following equations
(for one-way shear in SI units):

$$V_c = 0.035\lambda\phi_c \left(f'_c \rho_f E_f \frac{V_f}{M_f} d \right)^{1/3} b_w d \quad (8a)$$

$$0.1\lambda\phi_c \sqrt{f'_c} b_w d \leq V_{c,f} \leq 0.2\lambda\phi_c \sqrt{f'_c} b_w d \quad (8b)$$

$$\frac{V_f}{M_f} \leq 1.0 \quad (8c)$$

where b_w = width of the web; ϕ_c = resistance factor for concrete; M_f = moment at section of interest; V_f = shear at section of interest; d = distance from extreme compression fiber to neutral axis at balanced strain condition; λ = factor reflecting concrete density effect. For sections with an effective depth greater than 300 mm (11.8 in.) and with no transverse shear reinforcement or less transverse reinforcement than the minimum required by code; the value of V_c is calculated using the following equation:

$$V_c = \left(\frac{130}{1000 + d} \right) \lambda \phi_c \sqrt{f'_c} b_w d \geq 0.08 \lambda \phi_c \sqrt{f'_c} b_w d \quad (9)$$

d) Shear prediction proposed by El-Sayed et al. (2006a) in SI units

$$V_c = \left(\frac{\rho_f E_f}{90 \beta_1 f'_c} \right)^{1/3} \left(\frac{\sqrt{f'_c}}{6} b_w d \right) \leq \frac{\sqrt{f'_c}}{6} b_w d \quad (10)$$

4.2.2 Failure Mode and Experimental Shear Strength of Panels

A summary of test results for six specimens is shown in Table 3; these include deflection measured at midspan, shear strength of the specimen (dead load of the specimen was included), ratio of experimental shear strength to different shear strength values predicted by ACI 440.1R (2006), JSCE (1997), CAN/CSA (2002), and the equation proposed by El-Sayed et al. (2006a). Table 3 also lists the ratio of experimental shear strength to the prediction proposed in this report, which will be discussed in Section 4.2.3. All specimens had initial cracks due to lifting and transportation of concrete deck panels. Table 3 shows that ACI 440.1R-06 is very conservative compared to the other three predictions. Comparing the prediction of lightweight concrete to normal weight concrete, the lightweight concrete prediction is not as conservative as the normal weight concrete, especially using ACI 440.1R-06 equations.

The load versus midspan deflection behavior is shown in Figures 17-19. Generally the load deflection diagram is bilinear. The stiffness of the panels is much lower after reaching the cracking moment for both normal weight and lightweight concrete specimens. Before the cracking moment, the stiffness of lightweight concrete panels was approximately the same as that of the normal weight panels; after reaching the cracking moment, normal weight panels had a higher stiffness than lightweight panels. As far as the value of ultimate shear strength, the normal weight concrete panels achieved a higher shear strength compared to lightweight concrete panels. The experimental shear strength of lightweight concrete panels was about 84% that of normal weight concrete panels.

Table 3. Summary of Test Results

Specimen	Deflection (in.)	Shear strength V_{exp} (kips)	$\frac{V_{exp}}{V_{ACI}}$	$\frac{V_{exp}}{V_{JSCE}}$	$\frac{V_{exp}}{V_{CSA}}$	$\frac{V_{exp}}{V_{Sayed}}$	$\frac{V_{exp}}{V_{prop}}$	Initial crack width (in.)
1-NW-B2	1.698	27.58	2.10	1.55	1.75	1.56	2.10	0.002
2-LW-B1	1.064	22.92	1.46	1.30	1.36	1.26	1.72	0.005
3-NW-B2	1.649	27.70	1.93	1.46	1.58	1.40	1.93	0.002
4-LW-B2	1.408	23.28	1.47	1.24	1.34	1.19	1.73	0.003
5-NW-B2	2.638	72.71	1.89	1.39	1.58	1.40	1.89	0.002
6-LW-B1	1.832	61.32	1.40	1.18	1.32	1.18	1.65	0.005

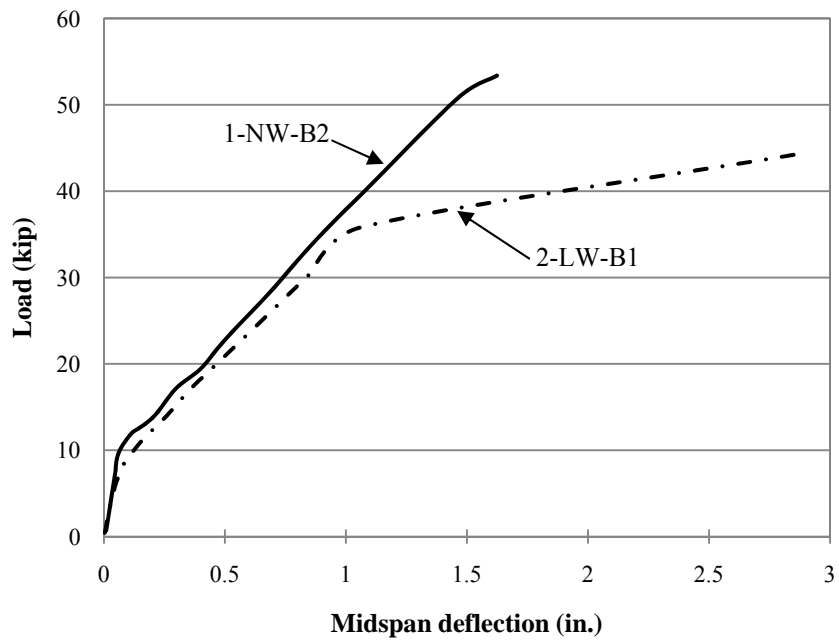


Figure 17. Load deflection diagram for 2 ft x 12 ft specimens

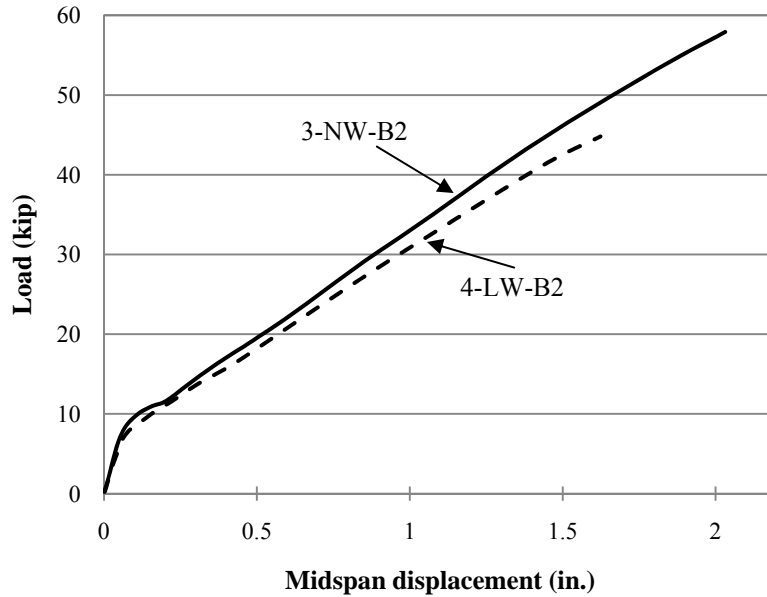


Figure 18. Load deflection diagram for 2 ft x 13 ½ ft specimens

The 2 ft wide precast concrete panels failed suddenly but not catastrophically, with a diagonal crack forming across the width of the specimen near one of the two supports; the diagonal tension failure mode was identical for normal weight and lightweight concrete panels as shown in Figure 20. Shortly after the formation of the critical crack, the concrete split along the bottom and top mat of GFRP bars due to debonding. However, this failure mode is not considered catastrophic because after reaching the ultimate load, the cracked panels could still support approximately half of the ultimate load through catenary action of the top and bottom GFRP mats. For the 6 ft wide panels, the diagonal crack formed initially on one side of the specimen through half of the specimen's width of 6 ft, as shown in Figure 21. At failure, the diagonal crack grew across the entire 6 ft width. Comparing Figures 20 and 21, it can be seen that the failure pattern was similar for both 2 ft wide and 6 ft wide panels; both failed in a diagonal tension failure mode.

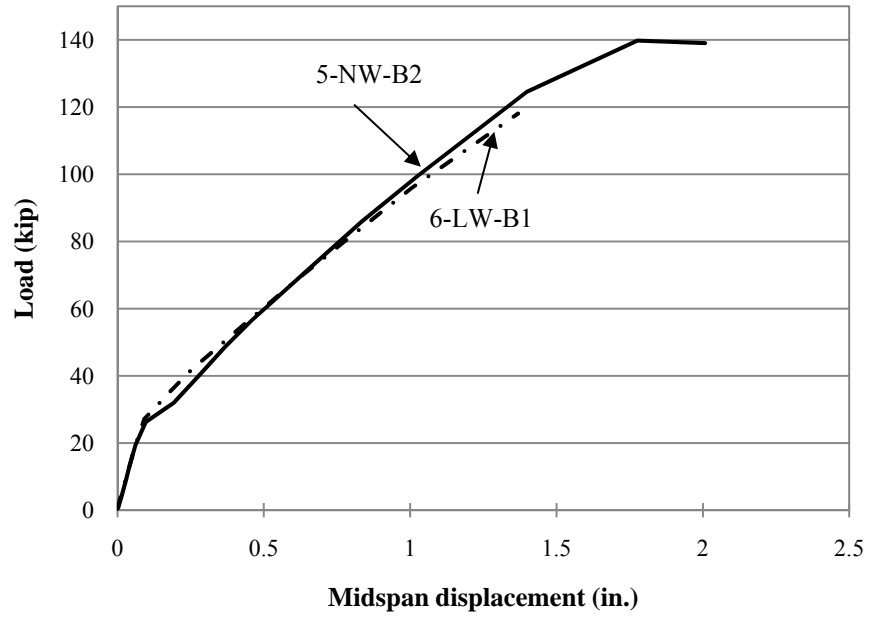


Figure 19. Load deflection diagram for 6 ft x 12 ft specimens



Figure 20. Failure of 2 ft wide panels: (a) NW GFRP panel, (b) LW GFRP panel



(a)



(b)

Figure 21. Failure of 6 ft wide panels: (a) NW GFRP panel, (b) LW GFRP panel

4.2.3 Recommendation for Modification of the ACI 440.1R-06 Shear Equation

Failure of all specimens is classified as one-way shear failure. ACI 440.1R specifies that the one-way shear strength of FRP reinforced flexural members is:

$$V_c = 5\sqrt{f'_c}b_w c \quad (\text{lbs}) \quad (11a)$$

$$c = kd \quad (11b)$$

$$k = \sqrt{2\rho_f n_f + (\rho_f n_f)^2} - \rho_f n_f \quad (11c)$$

$$E_c = \left[40,000\sqrt{f'_c} + 10^6 \right] \left(\frac{w_c}{145} \right)^{1.5} \quad (11d)$$

where f'_c = specified compressive strength of concrete (psi); b_w = width of the web (in.);
 c = cracked transformed section neutral axis depth, (in.); d = distance from extreme compression fiber to centroid of tension reinforcement, (in.); n_f = ratio of modulus of elasticity of FRP bars to

modulus of elasticity of concrete; k = ratio of depth of neutral axis to reinforcement depth;
 E_c = modulus of high-strength concrete (psi); w_c = concrete unit weight (pcf).

Table 3 gives the maximum shear strength at failure obtained in the experiments, and the ratio of ultimate shear strength calculated from the experiments to the shear strength predicted using different codes and equations proposed by other researchers. From Table 3, it is clear that in the case of the ACI 440.1R-06 guidelines, the shear strength ratio for normal weight concrete panels was higher than the shear strength ratio for lightweight concrete panels. This is because the ACI 440.1R-06 design guidelines do not include any specific provisions for the prediction of shear capacity for lightweight concrete panels reinforced with GFRP bars; Eq. (11) was used for both normal weight and lightweight concrete panels.

A reduction factor for one-way shear is introduced herein to consider the effect of lightweight concrete on the shear strength of concrete panels reinforced with GFRP bars. A reduction factor, which is defined as λ in the ACI 318 (2008) Building Code Requirements, is introduced into Eq. (11a) to obtain a modified equation considering the lightweight concrete as:

$$V_c = 5\lambda\sqrt{f'_c}b_wc \quad (\text{lbs}) \quad (12)$$

In the ACI 318 Building Code (2008), the reduction factor λ is equal to 0.85 for sand-lightweight concrete reinforced with steel bars. To determine the applicability of this reduction factor, a database of 97 beams and one-way slabs reinforced with GFRP bars that were tested by various researchers has been established, including the deck panels tested in this research. No GFRP or steel stirrups were used in any of the 97 tests; all the tested specimens were reinforced with GFRP bars and failed in a diagonal tension shear or compression shear failure mode.

Figure 22 shows the experimental shear strength normalized by the shear strength equation from the ACI 440.1R-06 design guidelines (Eq. (11a)). The average shear strength for normal weight concrete specimens from all experiments had higher reserve strength than that of lightweight concrete specimens. Figure 23 shows the experimental shear strength normalized by the shear prediction equation proposed in this research (Eq. (12)), using an extended database from tests carried out using normal weight concrete by Swamy and Aburawi (1997), Deitz et al.

(1999), Alkhrdaji et al. (2001), Yost et al. (2001), Tureyen and Frosch (2002), Gross et al. (2003), Ashour (2005), El-Sayed et al. (2005, 2006(a), 2006(b)), Alam and Hussein (2009), Jang et al. (2009), and Bentz et al. (2010). To achieve the same ratio of experimental shear strength to predicted shear strength for both normal weight and lightweight concrete panels reinforced with GFRP bars, a reduction factor of $\lambda=0.80$ was used in Figure 23. The properties of panels in the extended database of specimens tested by the researchers and a comparison of different shear prediction equations are shown in Appendix B and Appendix C, respectively.

Using the ACI 440.1R-06 shear prediction equation, the average ratio of experimental to predicted shear strength calculated from the database is equal to 1.91 for normal weight panels and 1.50 for lightweight panels; the standard deviation is 33% for normal weight panels and 10% for lightweight panels. The ratio of experimental to predicted shear strength is smaller for lightweight concrete panels compared to normal weight concrete panels. Using a reduction factor λ of 0.80 and the proposed equation (Eq. 12), the average of the ratio of experimental shear strength to calculated shear strength is 1.88 for lightweight concrete panels, with a standard deviation of 13%. The ratio of experimental to predicted shear strength for lightweight concrete panels in this case is close to that of normal weight concrete panels. The value of $\lambda =0.80$ is also supported by the split cylinder tests, in which the lightweight concrete had a lower tensile strength than normal weight concrete.

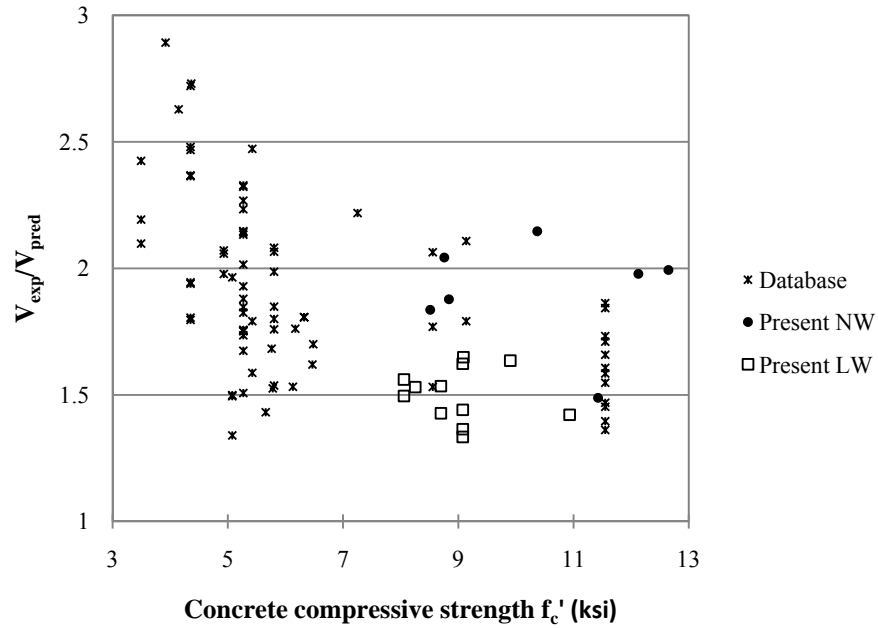


Figure 22. Experimental shear strength normalized by ACI 440 equation

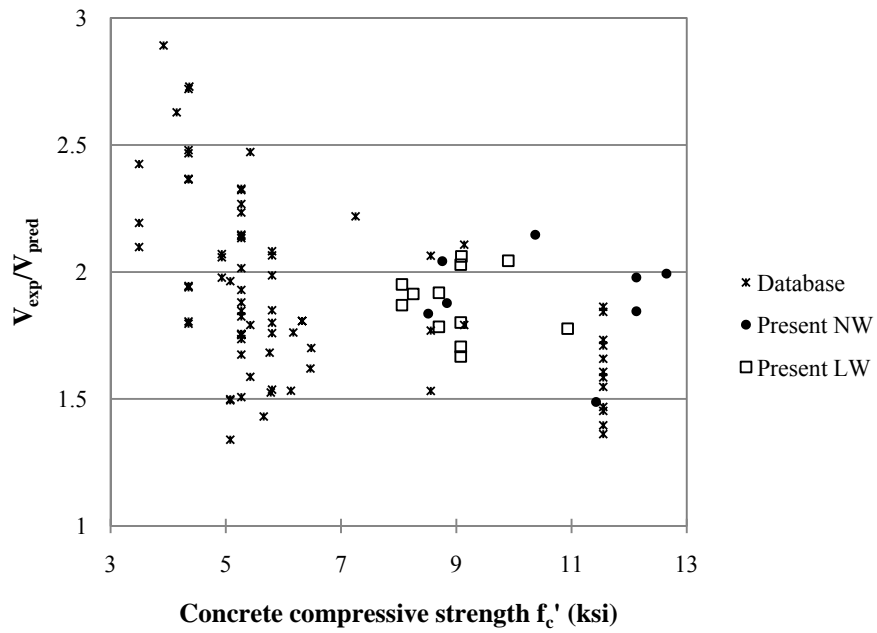


Figure 23. Experimental shear strength normalized by modified equation Eq. (12)

4.3 Deflection of Deck Panels

The panels were designed using ACI 440.1R-06 for service loads. Deflection was calculated using the effective moment of inertia I_e from ACI 440.1R with an allowable service load deflection equal to (span/800) according to AASHTO (2007) deflection requirements for deck panels.

4.3.1 Deflection Prediction in ACI 440.1R-06

Due to the lower modulus of elasticity of FRP bars, FRP reinforced members with an identical reinforcement ratio to steel reinforced members tend to have larger deflections compared to steel reinforced members. ACI 440.1R-06 requires the use of a direct method of deflection control. Before the concrete member cracks, the gross moment of inertia I_g is used to calculate the member deflection. After the cracking moment is reached, the effective moment of inertia should be used to calculate member deflection. The effective moment of inertia is given in ACI 440.1R-06 as:

$$I_e = \left(\frac{M_{cr}}{M_a} \right)^3 \beta_d I_g + \left[1 - \left(\frac{M_{cr}}{M_a} \right)^3 \right] I_{cr} \leq I_g \quad (13a)$$

$$\beta_d = \frac{1}{5} \left(\frac{\rho_f}{\rho_{fb}} \right) \quad (13b)$$

where I_e = effective moment of inertia; I_{cr} = moment of inertia of transformed cracked section; I_g = gross moment of inertia; β_d = reduction coefficient used in calculating deflection; M_{cr} = cracking moment; M_a = maximum moment in the member at stage at which deflection is computed.

The deflection predicted by Eq. (14) using the effective moment of inertia from ACI 440.1R-06 was calculated for the panels as shown in Figure 24. The panels were simply

supported on two concrete beams; the distributed load on the steel bearing plate is equal to the load recorded from the actuator divided by the steel bearing plate length; $q = P/S$, S = steel bearing plate length. The following equations are used:

$$M_{(x)} = \frac{P}{2}x \quad 0 < x < \frac{L-S}{2} \quad (14a)$$

$$M_{(x)} = \frac{P}{2}x - \frac{q\left(x - \frac{L-S}{2}\right)^2}{2} \quad \frac{L-S}{2} < x < \frac{L}{2} \quad (14b)$$

$$m_{(x)} = \frac{1}{2}x \quad 0 < x < \frac{L}{2} \quad (14c)$$

$$\Delta = \int_0^L \frac{M_{(x)}m_{(x)}}{EI_e} dx \quad (14d)$$

where, $M_{(x)}$ = moment from the left side support; P = load recorded from the actuator; $m_{(x)}$ = moment from unit load; Δ = calculated deflection. The deck panels and loading conditions were symmetric, thus the total deflection equals two times the value given by Eq. (14d) when integrating from 0 to $L/2$.

The deflection predicted by Eq. (14) using the effective moment of inertia from the ACI 440.1R-06 guidelines and the actual deflections measured in the experiments under service and ultimate load are given in Table 4. The measured deflections under service and ultimate load for an extended database of specimens tested by the researchers are shown in Appendix D. Table 4 shows that at service load, the deflection predicted by Eq. (14) is much smaller than the experimental deflection. The deflection predicted by Eq. (14) at ultimate load is close to the experimentally measured deflection; with the exception of panel 5-NW-B2 all other predicted deflections were within 10% of the measured deflections. The numbers shown in Table 4 indicate that the ACI 440.1R-06 guidelines predict a much higher effective moment of inertia under service load than that observed in the tests; however, the effective moment of inertia predicted by ACI 440.1R-06 under ultimate load is close to that of the test specimens.

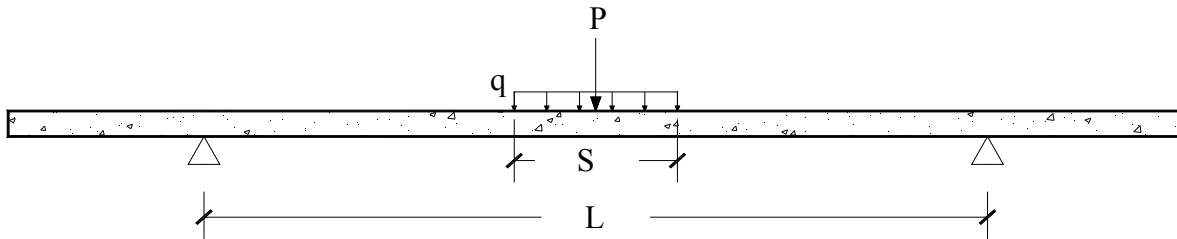


Figure 24. Deflection prediction

Table 4. Deflection of Panels at Service and Ultimate Load

Specimen	Service load		Ultimate load	
	$\Delta_{\text{experiment}}$ (in.)	$\Delta_{\text{prediction}}$ (in.)	$\Delta_{\text{experiment}}$ (in.)	$\Delta_{\text{prediction}}$ (in.)
1-NW-B2	0.048	0.017	1.624	1.660
2-LW-B1	0.066	0.029	1.062	1.094
3-NW-B2	0.057	0.018	2.032	2.140
4-LW-B2	0.068	0.023	1.624	1.689
5-NW-B2	0.074	0.017	2.008	1.434
6-LW-B1	0.069	0.021	1.368	1.240

4.3.2 Deflection Requirements in the AASHTO LRFD Bridge Design Specifications

In the AASHTO LRFD Bridge Design Specifications (2007), an HL-93 live load is used for design. The HL-93 live load consists of a design truck or tandem, combined with a design lane load. For the 2 ft wide specimens only one set of wheels could possibly be placed on the panel with a load equal to 16 kips; for the 6 ft wide specimens, two sets of wheels from the tandem could possibly be placed on the panel with a load equal to 25 kips. The design lane load is a uniform load of 640 lbs per linear foot of load lane. GFRP bars have a higher tensile strength than that of steel bars but a much smaller modulus of elasticity; typically, service load deflection and crack width control the design of GFRP reinforced members. Figure 25 shows the moment-deflection diagram and the deflection requirement at service load for 2 ft x 12 ft panels with an 8 ft span; Figure 26 shows the moment-deflection diagram and the deflection requirement at service load for 2 ft x 13 ½ ft panels with a 9 ½ ft span; Figure 27 shows the moment-deflection comparison for 6 ft x 12 ft panels with an 8 ft span. Figure 28 shows the moment-deflection comparison of 2 ft x 12 ft and 2 ft x 13 ½ ft deck panels. In the figures, lightweight concrete and

normal weight concrete panels have different service moments because of the difference in dead load. Only the normal weight concrete panel service load moments are shown in the figures since they are larger than those corresponding to the lightweight concrete panel. According to the AASHTO LRFD Bridge Design Specifications (2007), the service moments and deflection are calculated using the following equations:

$$M_{DL} = \frac{DL \cdot S^2}{10} \tag{15a}$$

$$M_{LL} = \frac{S + 2}{32} P \tag{15b}$$

$$\Delta = \frac{L}{800} \tag{15c}$$

where, M_{DL} = dead load moment per foot-width of slab, (ft-lbs); M_{LL} = live load moment per foot-width of slab, (ft-lbs); DL = dead load per foot width of slab, (lbs/ft); S = effective span length, (ft); P = live load, which equals 16 kips for the HL-93 truck load, and 25 kips for the tandem load; Δ = deflection, (in.); L = span length, (in.). Equation (15c) is the deflection limit of the panels.

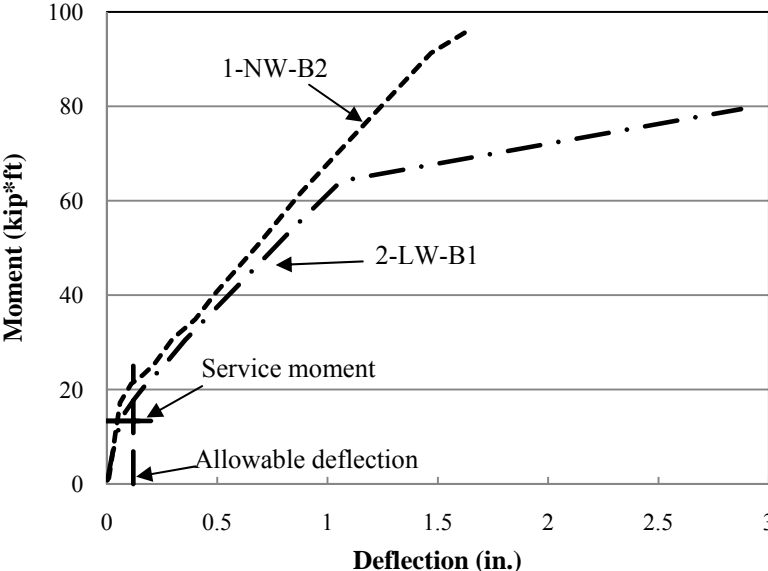


Figure 25. Deflection requirement under service moment for 2 ft x 12 ft panels

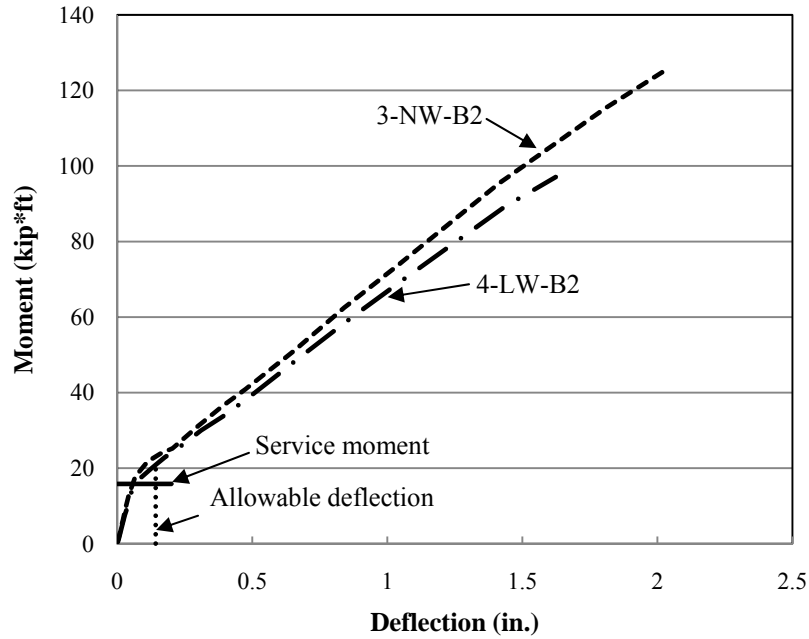


Figure 26. Deflection requirement under service moment for 2 ft x 13 ½ ft panels

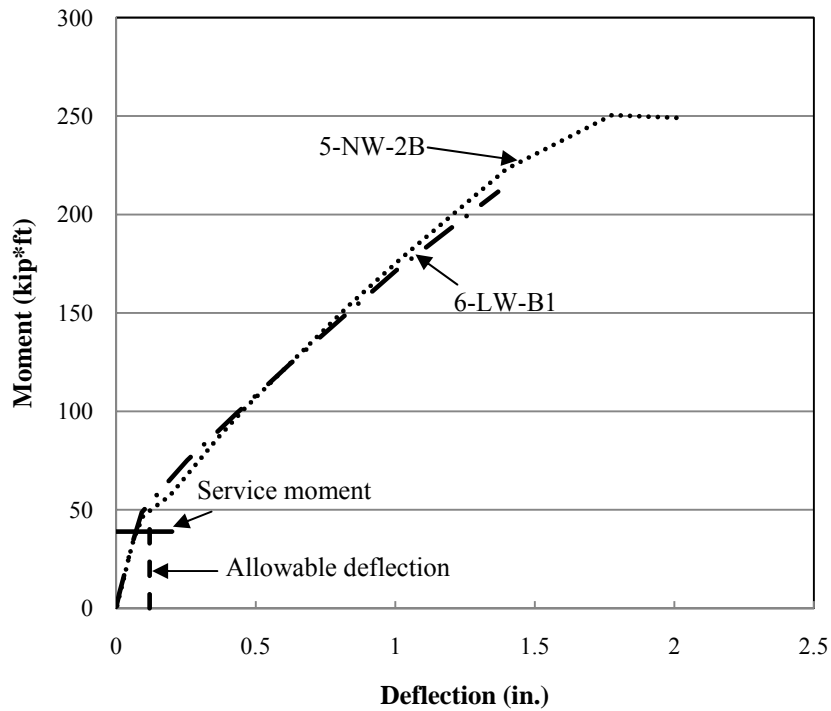


Figure 27. Deflection requirement under service moment for 6 ft x 12 ft panels

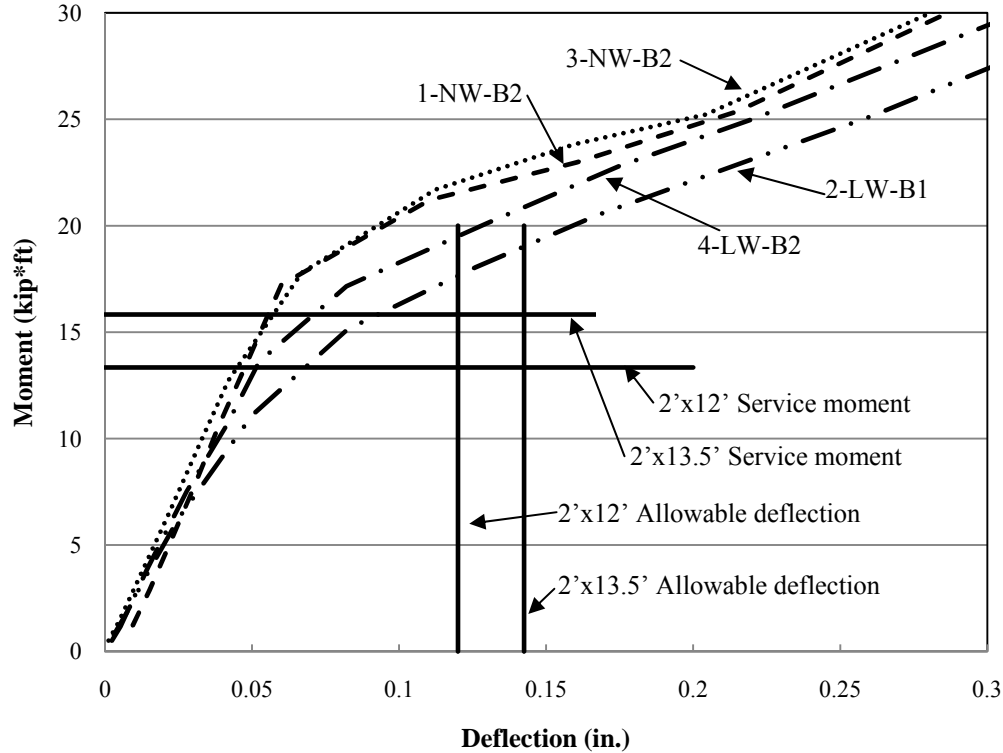


Figure 28. Deflection requirement under service moment: comparison of 2 ft x 12 ft panels with 2 ft x 13 ½ ft panels

Figures 25-28 show that the specimens satisfy the deflection requirement under the service moment which includes the dead load and live load moment. In Figures 25-28, normal weight concrete panels had larger service moments than lightweight concrete panels, and only the higher service moments are shown in the figures. The deflection requirements and the percentage of allowable deflection are shown in Table 5; the deflections under service moment observed in the tests are less than the values allowed by the AASHTO LRFD Bridge Design Specifications.

Table 5. Deflection under Service Load Moment Compared to the AASHTO LRFD Bridge Design Specifications

	2 ft x 12 ft				2 ft x 13 ½ ft				6 ft x 12 ft			
	1-NW-B2		2-LW-B1		3-NW-B2		4-LW-B2		5-NW-B2		6-LW-B1	
	Moment (kip*ft)	Defl. (in.)										
Service	13.34	0.120	13.12	0.120	15.83	0.143	15.51	0.143	38.97	0.120	38.31	0.120
Experiment		0.048		0.066		0.057		0.068		0.074		0.069
% of allowable deflection		40%		55%		40%		48%		62%		57%

5.0 CONCLUSIONS

This project has evaluated the performance of normal weight and lightweight concrete precast panels reinforced with GFRP bars. Three sets of specimens were built and tested. The first set of specimens and the third set of specimens had the same span (8 ft) which is smaller than the typical prestressed concrete girder spacing, with a slab thickness of 9 ¼ in. The second set of specimens had a typical prestressed concrete girder spacing (9 ½ ft) with an increased slab thickness of 10 ¾ in. The first and second set of specimens had the same width (2 ft) which simulates the behavior of a strip from the deck panel designed using the strip method; the third set of specimens had a larger width (6 ft), which is typical of actual bridge precast deck panels used at the Beaver Creek Bridge on US 6 in Utah (6 ft-10 in. x 41 ft-5 in. x 9 ¼ in.). All panels tested were simply supported which is a much more severe condition than the details used in actual precast bridge deck panels; the latter method attaches the precast panels to the girders using blockouts by anchoring the panels through grout and steel studs in the blockouts to the top face of the girder flanges; thus, the precast panels are continuous among different spans, which provides enough development length for the reinforcement to develop full strength.

Failure of both normal weight and lightweight concrete panels was sudden but not catastrophic; both types of specimens had a residual capacity after failure which was approximately equal to half the ultimate load. All specimens failed in a diagonal tension failure mode. Failure was initiated as a single diagonal crack, which lead to a shear failure and subsequent crushing of the concrete in the compression zone. No GFRP bars ruptured in the tensile zone region during any of the tests; a few top mat GFRP bars near the edge of some panels snapped and sheared off after the ultimate load was reached, shortly before the ultimate deflection was reached. The failure mode for lightweight and normal weight concrete deck panels was the same.

All specimens had a bilinear load deflection diagram. The stiffness of the specimens before the cracking moment was much higher than the stiffness after the cracking moment. Before the cracking moment was reached, both normal weight and lightweight concrete deck

panels had similar stiffness. After the cracking moment was reached, the normal weight concrete panels generally had a higher stiffness than lightweight concrete panels.

The 9 ½ ft span specimens with a 10 ¾ in. slab thickness worked equally as well compared to the 8 ft span specimens with a 9 ¼ in. slab thickness. Under service load, both 9 ½ ft and 8 ft span specimens satisfied the AASHTO LRFD Bridge Design Specification deflection requirements. All of the 2 ft wide specimens had a deflection ratio of 40% of the allowable deflection under service load. The 6 ft wide specimens had a larger deflection but the deflection ratio was still only 55% of the allowable deflection under service load.

Normal weight concrete deck panels reinforced with GFRP bars achieved 1.89 to 2.10 times the shear capacity predicted by the ACI 440.1R-06 one-way shear equation. Currently, ACI 440.1R-06 guidelines do not provide any specification regarding the use of lightweight concrete reinforced with GFRP bars. Using the same equation for lightweight concrete as for normal weight concrete, the lightweight concrete deck panels reinforced with GFRP bars achieved 1.40 to 1.47 times the shear capacity predicted by ACI 440.1R-06. Using the present tests and additional results from recent research, a modified ACI 440.1R-06 one-way shear prediction equation was proposed in this report; it was found that a modification factor (λ) equal to 0.80, yields a predicted shear capacity of lightweight concrete deck panels that has approximately the same ratio of experimental to predicted shear strength as the shear capacity predicted for normal weight concrete deck panels.

6.0 RECOMMENDATIONS AND IMPLEMENTATION

The results of the tests carried out in this research project are sufficient to recommend the use of lightweight concrete reinforced with GFRP bars for construction of precast concrete bridge decks. Both normal weight and lightweight concrete panels had a residual capacity after failure which was approximately equal to one-half the ultimate load capacity. The research has also shown that there is a choice for the designer when it comes to meeting the AASHTO LRFD Bridge Design Specifications deflection requirement. The first option is to keep the slab thickness at 9 ¼ in. and reduce the deck span from 9 ½ ft to 8 ft; this option involves the addition of new girder lines. The second option is to keep the deck span at 9 ½ ft and increase the slab thickness to 10 ¾ in. Bridge decks using the Accelerated Bridge Construction method could benefit from the use of GFRP reinforced lightweight concrete precast panels. In addition, deflections measured at service loads were less than the allowable deflections permitted by the AASHTO LRFD Bridge Design Specifications. Implementation with a smaller GFRP reinforcement ratio would be more economical and should include the use of lightweight concrete with the appropriate modification factor for shear strength capacity found in this research. The Beaver Creek Bridge on US 6 near Price, Utah, has used GFRP reinforcement in normal weight concrete deck panels and was constructed in September 2009. The deck span used was 7 ft-7 in.; the bridge deck with a 9 ¼ in. thickness slab has performed very well to date. Further implementation of lightweight concrete or normal weight precast concrete panels for bridge decks reinforced with GFRP bars is recommended based on the results of this research project.

THIS PAGE INTENTIONALLY LEFT BLANK

APPENDIX A. LIGHTWEIGHT CONCRETE MIX DESIGN

Material	Unit	Moi. %	Mix.	Target	Actual	Alarm	Deviation %	Actual					
								SSD lbs/Y3	Water lbs/Y3	Dens. lbs/Y3	SSD %		
Holcim Type 2	lbs		527	1055	1055		0	0.0	602.5	602.5	0.0	5299	113.7
Type F Fly Ash	lbs		131	265	265		0	0.0	151.3	151.3	0.0	3970	38.1
Point Sand	lbs	1.9	1188	2415	2420		5	0.2	1382.1	1356.3	25.8	4119	329.3
Utelite	lbs	0.0	989	1980	1974		-6	-0.3	1127.4	1127.4	0.0	3170	355.6
MBAE-90	Ounce	89.0	3.50	7.00	6.75		-0.25	-57.1	0.2	0.0	0.2	2965	0.0
Glenium 30-30	Ounce	60.0	80	160	160		0	0.0	5.7	2.3	3.4	1912	1.2
Cold Water	lbs		227	410	409		-1	-0.2	233.6	0.0	233.6	1685	0.0
Cold Water	lbs		0	0	18		18	0.0	10.3	0.0	10.3	1685	0.0
Total	lbs		3067	6135	6151				3513.1	3239.8	273.3		837.9

	Mix.	Target	Actual	Unit	Deviation		%
					%		
SSD		1.468	1.467	Y3	-0.001	0.0	837.9
Air (0.0%)	0.000	0.000	0.000	Y3	0.000	0.0	0.0
Water added		0.243	0.253	Y3	0.010	4.1	144.6
Total moisture		0.030	0.031	Y3	0.000	0.2	17.4
Total		1.742	1.751	Y3	0.009	0.5	999.9
W/C	0.350	0.350	0.362		0.012	3.4	
Total water/powder ratio		0.350	0.360		0.010	2.9	
Max. water	0.3			Y3			
Water/concrete		7.5	7.8		0.3	3.4	
Total mixing time	90	90	206	Sec.	116	128.9	
Final mixing time	16	16	150	Sec.	134	837.5	
Wattmeter idling			50				
Wattmeter end value			64				
Mortar content	0.56	1.12	1.13	Y3	0.011	1.0	
Filler Content	1848.02	3694.02	3698.92	lbs	4.91	0.1	

APPENDIX B. PROPERTIES OF SLABS USED FOR DETERMINATION OF λ

	Specimen	f_c'	E_c	f_u	E_t	b_w	h	d	a/d	Span	β₁	ρ_t	ρ_t/ρ_b	k	c
		psi	ksi	ksi	ksi	in.	in.	in.		in.					in.
Present research	#8 B1NW	11420	5280	104	6280	25.00	10.75	9.44	6.04	114	0.650	0.0079	0.75	0.124	1.17
	#9 B2NW	8840	4760	104	6280	25.00	10.75	9.44	6.04	114	0.650	0.0079	0.97	0.131	1.23
	#1 B1NW	10370	5070	104	6280	25.00	9.25	7.94	6.05	96	0.650	0.0094	0.99	0.137	1.09
	#2 N2NW	12650	5500	104	6280	25.00	9.25	7.94	6.05	96	0.650	0.0094	0.81	0.132	1.05
	#3 N2NW	8760	4740	104	6280	25.00	9.25	7.94	6.05	96	0.650	0.0094	1.17	0.142	1.12
	#12 B1NW	12130	5400	104	6280	73.00	9.25	7.94	6.05	96	0.650	0.0096	0.87	0.135	1.07
	#13 B2NW	8510	4690	104	6280	73.00	9.25	7.94	6.05	96	0.650	0.0096	1.24	0.144	1.14
	#18 B1NWE	12130	5400	104	6280	73.00	9.25	7.94	6.05	96	0.650	0.0054	0.48	0.103	0.81
	#10 B1LW	9080	3760	104	6280	25.00	10.75	9.44	6.04	114	0.650	0.0079	0.95	0.146	1.37
	#11 B2LW	8700	3700	104	6280	25.00	10.75	9.44	6.04	114	0.650	0.0079	0.99	0.147	1.39
	#4 B1LW	9090	3760	104	6280	25.00	9.25	7.94	6.05	96	0.650	0.0094	1.13	0.158	1.25
	#5 B1LW	10930	4050	104	6280	25.00	9.25	7.94	6.05	96	0.650	0.0094	0.94	0.152	1.21
	#6 B2LW	8700	3700	104	6280	25.00	9.25	7.94	6.05	96	0.650	0.0094	1.18	0.159	1.26
	#7 B1LW	9900	3890	104	6280	25.00	10.25	8.94	4.48	80	0.650	0.0083	0.92	0.147	1.31
	#14 B1LW	9080	3760	104	6280	73.00	9.25	7.94	6.05	96	0.650	0.0096	1.16	0.160	1.27
	#15 B1LW	9080	3760	104	6280	73.00	9.25	7.94	6.05	96	0.650	0.0096	1.16	0.160	1.27
	#16 B2LW	8250	3620	104	6280	73.00	9.25	7.94	6.05	96	0.650	0.0096	1.27	0.162	1.29
	#17 B2LW	8060	3590	104	6280	73.00	9.25	7.94	6.05	96	0.650	0.0096	1.30	0.163	1.29
	#19 B1LWE	9080	3760	104	6280	73.00	9.25	7.94	6.05	96	0.650	0.0054	0.64	0.122	0.97
	#20 N2LWE	8060	3590	104	6280	73.00	9.25	7.94	6.05	96	0.650	0.0054	0.72	0.124	0.99

**APPENDIX C. COMPARISON AND VERIFICATION OF DIFFERENT SHEAR
PREDICTION EQUATIONS**

	Specimen	f_c'	V_{exp}	V_{exp}/V_{ACI}	V_{exp}/V_{ACI-M}	$V_{exp}/V_{CAN/CSA}$	V_{exp}/V_{JSCE}	$V_{exp}/V_{El-Sayed}$
		psi	ksi					
Present research	#8 B1NW	11420	24.01	1.53	1.53	1.24	1.25	1.16
	#9 B2NW	8840	27.95	1.93	1.93	1.58	1.46	1.40
	#1 B1NW	10370	30.62	2.21	2.21	1.84	1.72	1.68
	#2 N2NW	12650	30.26	2.05	2.05	1.70	1.70	1.61
	#3 N2NW	8760	27.62	2.10	2.10	1.75	1.55	1.56
	#12 B1NW	12130	87.63	2.03	2.03	1.69	1.67	1.59
	#13 B2NW	8510	72.74	1.89	1.89	1.58	1.39	1.40
	#18 B1NWE	12130	62.09	1.90	2.23	1.46	1.44	1.37
	#10 B1LW	9080	22.44	1.37	1.61	1.25	1.17	1.12
	#11 B2LW	8700	23.69	1.47	1.73	1.34	1.24	1.19
	#4 B1LW	9090	25.26	1.69	1.99	1.58	1.42	1.42
	#5 B1LW	10930	23.09	1.46	1.72	1.36	1.30	1.26
	#6 B2LW	8700	23.18	1.58	1.85	1.48	1.30	1.31
	#7 B1LW	9900	27.46	1.68	1.98	1.40	1.47	1.40
	#14 B1LW	9080	61.76	1.40	1.65	1.32	1.18	1.18
	#15 B1LW	9080	65.23	1.48	1.74	1.39	1.24	1.24
	#16 B2LW	8250	67.21	1.57	1.85	1.48	1.28	1.30
	#17 B2LW	8060	68.01	1.60	1.89	1.51	1.30	1.32
	#19 B1LWE	9080	56.03	1.67	1.96	1.45	1.30	1.30
	#20 N2LWE	8060	49.71	1.54	1.81	1.34	1.15	1.18

APPENDIX D. DEFLECTION OF PANELS AT SERVICE AND ULTIMATE LOAD

Specimen	Service load		$\Delta_{\text{prediction}}$ design concrete strength 6000 psi (in.)	Ultimate load		$\Delta_{\text{prediction}}$ using design concrete strength 6000 psi (in.)
	$\Delta_{\text{experiment}}$ (in.)	$\Delta_{\text{prediction}}$ (in.)		$\Delta_{\text{experiment}}$ (in.)	$\Delta_{\text{prediction}}$ (in.)	
#1 B1NW	0.079	0.016	0.020	1.486	1.839	1.795
#2 B2NW	0.040	0.015	0.020	1.719	1.802	1.869
#3 B2NW	0.048	0.017	0.020	1.624	1.660	1.693
#4 B1LW	-	-	-	-	-	-
#5 B1LW	0.066	0.020	0.025	2.874	1.390	1.438
#6 B2LW	-	-	-	-	-	-
#7 B1LW	-	-	-	-	-	-
#8 B1NW	0.120	0.016	0.021	1.633	1.645	1.694
#9 B2NW	0.057	0.018	0.021	2.031	2.140	2.174
#10 B1LW	0.074	0.022	0.026	1.524	1.588	1.619
#11 B2LW	0.068	0.023	0.026	1.624	1.689	1.719
#12 B1NW	0.071	0.015	0.020	2.054	1.745	1.806
#13 B2NW	0.074	0.017	0.020	2.008	1.434	1.463
#14 B1LW	0.069	0.021	0.025	1.368	1.240	1.272
#15 B1LW	0.108	0.021	0.025	1.536	1.320	1.353
#16 B2LW	0.110	0.022	0.025	2.631	1.091	1.116
#17 B2LW	0.072	0.022	0.025	1.222	1.393	1.417
#18 B1NWE	0.063	0.015	0.020	2.430	2.023	2.103
#19 B1LWE	0.143	0.021	0.025	2.088	1.886	1.928
#20 B2LWE	0.146	0.022	0.025	1.920	1.638	1.669

REFERENCES

Alam, M.S., Hussein, A., (2009). "Shear strength of concrete beams reinforced with Glass Fiber Reinforced Polymer (GFRP) bars." Proc. 9th Int. Symposium on Fiber Reinforced Polymer Reinforcement for Reinforced Concrete Structures, FRPRCS-9, Sydney, Australia.

Alkhrdaji, T., Wideman, M., Belarbi, A., and Nanni, A., (2001). "Shear Strength of GFRP RC Beams and Slabs." Proceedings, Composites in Constructions, J. Figueiras, L. Juvandes, and R. Faria, eds., Balkema, Lisse, Netherlands, 409-414.

American Association of State Highway and Transportation Officials, (AASHTO) (2007). "LRFD Bridge Design Specifications." 4th Edition, Washington, D.C. 1526 pp.

American Association of State Highway and Transportation Officials, (AASHTO) (2009). "AASHTO LRFD Bridge Design Guide Specifications for GFRP Reinforced Concrete Decks and Traffic Railings." 1st Edition, Washington, D.C., 68 pp.

ACI Committee 318, (1999). "Building Code Requirements for Structural Concrete (ACI 318-99)," American Concrete Institute, Farmington Hills, Mich., 369 pp.

American Concrete Institute, ACI Committee 318, (2008). "Building Code Requirements for Structural Concrete (ACI 318-08) and Commentary (318 R-08)." Farmington Hills, MI, 430 pp.

American Concrete Institute, (ACI 440.1R-01), (2001). "Guide for the Design and Construction of Structural Concrete Reinforced with FRP Bars." American Concrete Institute, Farmington Hills, Mich.

American Concrete Institute, (ACI 440.1R-03), (2003). "Guide for the Design and Construction of Structural Concrete Reinforced with FRP Bars." American Concrete Institute, Farmington Hills, Mich., 42 pp.

American Concrete Institute, (ACI 440.1R-06) (2006). "Guide for the Design and Construction of Structural Concrete Reinforced with FRP Bars." American Concrete Institute, Farmington Hills, MI, 44 pp.

American Society for Testing Materials, (2004). "ASTM C496/C496M Standard Test Method for Splitting Tensile Strength of Cylindrical Concrete Specimens." ASTM International, West Conshohocken, PA, 2004, DOI: 10.1520/C0496_C0496M-04E01, www.astm.org.

American Society for Testing Materials, (2009). "ASTM C39/C39M Standard Test Method for Compressive Strength of Cylindrical Concrete Specimens." ASTM International, West Conshohocken, PA, 2009, DOI: 10.1520/C0039_C0039M-09A, www.astm.org.

Ashour, A.F., (2005). "Flexural and shear capacities of concrete beams reinforced with GFRP bars." *Constr. Build. Mater.*, 20(10), 1005-1015.

Bentz, E.C, Massam, L., and Collins, M.P., (2010). "The shear strength of large concrete members with FRP reinforcement." *Journal of Composites for Construction*, accepted January, 28, 2010.

Canadian Standards Association, (CAN/CSA S806-02) (2002). "Design and Construction of Building Components with Fibre Reinforced Polymers." Canadian Standards Association, Rexdale, Ontario, Canada, 177 pp.

Castrodale, R.W., and Robinson, G.M. (2008). "Performance of lightweight concrete bridge decks." *Concrete Bridge Conference*, St. Louis, MO.

Deitz, D.H., Harik, I.E., and Gesund, H., (1999). "One-way slabs reinforced with Glass Fiber Reinforced Polymer reinforcing bars." *Proc. 4th Int. Symposium on Fiber Reinforced Polymer Reinforcement for Reinforced Concrete Structures, FRPRCS4*, Baltimore, MD, pp. 279-286.

El-Sayed, A., El-Salakawy, E., and Benmokrane, B., (2005). "Shear strength of one-way concrete slabs reinforced with Fiber-Reinforced Polymer composite bars." *Journal of Composites for Construction*, ASCE, Vol. 9, No.2, pp. 147-157.

El-Sayed, A.K., El-Salakawy, E.F. and Benmokrane, B., (2006a). "Shear strength of FRP-reinforced concrete beams without transverse reinforcement." *ACI Structural Journal*, V. 103, No.2, pp. 235-243.

El-Sayed, A.K., El-Salakawy, E.F. and Benmokrane, B., (2006b). "Shear capacity of high-strength concrete beams reinforced with FRP bars." *ACI Structural Journal*, V.103, No. 3, pp. 383-389.

Gross, S.P., Yost, J.R., Dinehart, D.W., Svensen, E., (2003). "Shear strength of normal and high strength concrete beams reinforced with GFRP bars." *High performance materials in bridges*, *Proceedings of the International Conference*, ASCE, Kona, Hawaii, 426-437.

Jang, H., Kim, M., Cho, J., and Kim, C., (2009). "Concrete shear strength of beams reinforced with FRP bars according to flexural reinforcement ratio and shear span to depth ratio." Proc. 9th Int. Symposium on Fiber Reinforced Polymer Reinforcement for Reinforced Concrete Structures, FRPRCS-9, Sydney, Australia.

Japan Society of Civil Engineers (JSCE), (1997). "Recommendation for Design and Construction of Concrete Structures Using Continuous Fiber Reinforcing Materials". Concrete Engineering Series No. 23, 325 pp.

Swamy, N., Aburawi, M., (1997). "Structural implications of using GFRP bars as concrete reinforcement." Non-Metallic (FRP) Reinforcement for Concrete Structures, proceedings of the third international symposium, Vol. 2, pp. 503-510.

Tureyen, A.K., and Frosch, R., (2002). "Shear tests of FRP-reinforced concrete beams without stirrups." ACI Structural Journal, V. 99, No. 4, pp. 427-434.

Yunovich, M., and Thompson, N. (2003). "Corrosion of highway bridges: Economic impact and control methodologies." ACI Concrete Int., 25(1), 52-57.

Yost, J.R., Gross, S.P., and Dinehart, D.W. (2001). "Shear strength of normal strength concrete beams reinforced with deformed GFRP bars". Journal of Composites for Construction, ASCE, V.5, No.4, pp. 263-275.

THIS PAGE INTENTIONALLY LEFT BLANK

ACRONYMS

AASHTO – American Association of State Highway and Transportation Officials;

ABC – Accelerated Bridge Construction;

ACI – American Concrete Institute;

AFRP – Aramid Fiber Reinforced Polymer;

CFRP – Carbon Fiber Reinforced Polymer;

CSA – Canadian Standards Association;

FRP – Fiber Reinforced Polymer;

GFRP – Glass Fiber Reinforced Polymer;

JSCE – Japan Society of Civil Engineers;

LRFD – Load and Resistance Factor Design;

LVDT – Linear Variable Differential Transducer.